

EFFECTS OF Y_2O_3 AND α -ZrP ADDITIVES ON LUBRICATION OF GREASE

A Thesis

by

CHUNG JWA KIM

Submitted to the Office of Graduate and Professional Studies of
Texas A&M University
in partial fulfillment of the requirements for the degree of

MASTER OF SCIENCE

Chair of Committee,
Committee Members,
Head of Department,

Hong Liang
Partha Mukerjee
Miladin Radovic
Andreas Polycarpou

August 2014

Major Subject: Mechanical Engineering

Copyright 2014 Chung jwa Kim

ABSTRACT

Development of novel additives in lubricants is a promising approach for high performance and energy saving devices. Those include automotive, marine, and wind turbines. In a wind turbine, the unplanned break-down rate of bearings caused by improper lubricants is 40% ~50%. The objective of this research is to 1) develop novel nanomaterials as grease additives, and 2) obtain understanding in tribological performances of the same. The research focuses on zirconium phosphate and yttrium oxide nanoparticles as additives in grease. Experimental approach is used to investigate the effects of those nanomaterials on lubrication of grease. Experiments such as tribological experiments at room and elevated temperatures, galling resistance tests, and characterization of worn surfaces will be conducted. Characterization includes optical microscope, interferometer, and scanning electron microscope (SEM). Results showed that the addition of nanoparticles induced reduction of coefficient of friction. In addition, the wear rate of the test samples was reduced by adding nanoparticles.

This research investigates the effects of nanoparticles with unique shape and structure and develops understating in mechanisms. The research results will be beneficial to the application of lubricants for high performance and efficiency.

This thesis contains six chapters. Chapter I is the background information about tribology and materials needed to understand this research. Chapter II describes the motivation and objectives. Chapter III discusses the experimental procedures and materials used in this research. Chapter IV and V present and discuss the results obtained

from yttrium oxide and zirconium phosphate, respectively. Chapter VI discusses the major conclusions obtained from the results and offers suggestions for future work.

ACKNOWLEDGEMENTS

I would like to thank my committee chair and adviser, Dr. Hong Liang, for all her support and guidance throughout the course of my research. I have also received a lot of help from Dr. Abraham Clearfield and guidance from the students in the Surface Science Research Group throughout my graduate studies. I would like to thank my committee members, Dr. Partha Mukerjee and Dr. Miladin Radovic for their support. I am also grateful for the scholarship awarded to me by the Korean Army.

Most importantly, I would like to thank my family, Pyung Sin, Hyunseo Kim, and parents, for all of their support throughout my academic career. They have made a lot of sacrifices throughout the years in my life so that I may reach my goal. I would not be where I am without them and I am extremely grateful.

NOMENCLATURE

NS	Nanosheet
NP	Nanoplatelet
OM	Optical Microscopy
SEM	Scanning Electron Microscopy
TEM	Transmission Electron Microscopy
AFM	Atomic Force Microscopy
RPM	Revolutions per Minute
CoF	Coefficient of Friction
Y ₂ O ₃	Yttrium oxide
ZrP	Zirconium phosphate

TABLE OF CONTENTS

	Page
ABSTRACT	ii
ACKNOWLEDGEMENTS	iv
NOMENCLATURE	v
TABLE OF CONTENTS	vi
LIST OF FIGURES	ix
LIST OF TABLES	xii
CHAPTER I INTRODUCTION	1
1. 1. Tribology	1
1. 1. 2. Friction	2
1. 1. 3. Wear	4
1. 2. Lubrication	7
1. 2. 1. Semi-liquid lubricant	8
1. 2. 2. Nanomaterials as additives in lubricant	12
1. 3. Potential application of the enhanced lubricant in a wind turbine	13
1. 3. 1. Necessity of the enhanced lubricants in a wind turbine	14
1. 3. 2. Potential savings with lubrication improvement in a wind turbine	16
CHAPTER II MOTIVATION AND OBJECTIVES	18
CHAPTER III EXPERIMENTAL DETAILS	19
3.1. Materials	19
3. 1. 1. Yttrium Oxide (Y_2O_3)	20
3. 1. 2. Zirconium phosphate (ZrP)	21
3. 1. 3. Reference grease	22
3. 1. 4. Substrate material	23
3. 1. 5. Sample preparation	24
3. 2. Tribometer experiments	24
3. 2. 1. Pin-on-disc tribometer experiment	25
3. 2. 2. High temperature tribometer experiment	26
3. 3. Galling experiments	27

3. 3. 1. Test procedure	28
3. 3. 2. Visual inspection	29
3. 3. 3. Data analysis.....	30
3. 4. Wear analysis	31
3. 4. 1. Optical microscope.....	31
3. 4. 2. Interferometer	32
3. 4. 3. Scanning Electron Microscopy	33
3. 4. 4. Evaluation of wear rate.....	33
CHAPTER IV EFFECTS OF Y_2O_3 AS ADDITIVES ON LUBRICATION OF GREASE	35
4. 1. Effects on frictional behavior.....	35
4. 1. 1. Dispersion of Y_2O_3 in grease.....	36
4. 1. 2. Effects on concentration.....	36
4. 1. 3. Effects of Y_2O_3 on frictional behavior of grease at room temperature	37
4. 1. 4. Effects on frictional behavior at high temperature	39
4. 2. Effects on wear.....	41
4. 2. 1. Analysis of wear scar and wear track on worn surfaces.....	41
4. 2. 2. Analysis of roughness on worn surface.....	43
4. 2. 3. Comparison of wear rate	44
4. 3. Effects on galling resistance.....	46
4. 3. 1. Visual inspection	46
4. 3. 1. Data analysis.....	47
4. 4. Mechanisms of Y_2O_3 NSs on lubrication of grease.....	49
CHAPTER V EFFECTS OF α -ZrP AS ADDITIVES ON LUBRICATION OF GREASE	51
5. 1. Effects on frictional behavior.....	51
5. 1. 1. Dispersion of α -ZrP in grease.....	51
5. 1. 2. Effects on concentration.....	52
5. 1. 3. Effects on frictional behavior at room temperature.....	53
5. 1. 4. Effects on frictional behavior at high temperature	55
5. 2. Effects on wear.....	57
5. 2. 1. Analysis of wear scar and wear track on worn surface	57
5. 2. 2. Analysis of roughness on worn surface.....	60
5. 2. 3. Comparison of wear rate	62
5. 3. Effects on galling resistance.....	64
5. 3. 1. Visual inspection	65
5. 3. 2. Data analysis.....	65
5. 4. Mechanism of α -ZrP NPs on lubrication of grease.....	67
CHAPTER VI CONCLUSION AND FUTURE RECOMMENDATIONS.....	71

6. 1. Conclusions	71
6. 2. Future recommendations	72
REFERENCES	73

LIST OF FIGURES

	Page
Figure 1. Various forces on two interacting bodies	3
Figure 2. Abrasive removal of one material by another.....	5
Figure 3. Adhesive removal of one material by another	6
Figure 4. Comparison of surface area-volume ratio according to size [35].....	12
Figure 5. Effect of nanoparticle shape [34].....	13
Figure 6. Grease is used at three points in a wind turbine[42].....	15
Figure 7. TEM (left) and AFM (right) images of Y_2O_3 NSs [46]	20
Figure 8. TEM (left) and AFM (right) images of α -ZrP NPs [49].....	21
Figure 9. Diagram of Inconel alloy 718 used for tribological test	23
Figure 10. Interferometer results show 20nm of the roughness average for a substrate..	24
Figure 11. Pin-on-disc tribometer (CSM Instrument).....	26
Figure 12. Diagram of atesting configuration for high temperature tribometer.....	27
Figure 13. API RP 7A1 used in galling test [51]	28
Figure 14. Digital optical microscope (VHX-600)	32
Figure 15. Interferometer (ZYGO NEW VIEW 600).....	33
Figure 16. Diagram of parameter to calculate a wear rate	34
Figure 17. OM images of the reference grease (left) and Y_2O_3 (right) at 1000x	36
Figure 18. Comparison of the CoF from different concentrations	37
Figure 19. Comparison of the CoF under different loads	38
Figure 20. Comparison of the CoF at different rotating speeds	39

Figure 21. Comparison of the CoF with increased temperature	40
Figure 22. OM images of the wear scar of the reference grease(left) and Y_2O_3 (right)...	41
Figure 23. OM images of wear track of the reference grease (up) and Y_2O_3 (down).....	42
Figure 24. Interferometer resultson the reference grease(left) and Y_2O_3 (right).....	43
Figure 25. Interferometer results onthe grease without (up) and with Y_2O_3 (down)	44
Figure 26. Comparison of wear rate	46
Figure 27. No galling traces on a substrate before (left) and after (right) experiment.....	47
Figure 28. Make-up and break-out versus rotation degree plot for Y_2O_3	48
Figure 29. Illustration of the role of Y_2O_3 NSsbetween sliding surfaces.....	50
Figure 30. OM images of the reference grease (left) and α -ZrP (right) at 1000x	52
Figure 31. Comparison of the CoF from different concentrations	53
Figure 32. Comparison of the CoF under different loads	54
Figure 33. Comparison of the CoF at different rotating speeds	55
Figure 34. Comparison of the CoF with increased temperature	56
Figure 35. OM images of the wear scar of the reference grease(left) and α -ZrP (right)..	57
Figure 36. OM images of wear track of the reference grease (up) and α -ZrP (down).....	58
Figure 37. Interferometer results on the reference grease (left) and α -ZrP (right).....	59
Figure 38. SEM images of wear track on the reference grease (up) and α -ZrP (down) ..	60
Figure 39. Interferometer results onthe grease without (up) and with α -ZrP (down)	61
Figure 40. Comparison of wear rate.....	63
Figure 41. Friction response for 2 hours in tribometer experiment	64
Figure 42. No galling traces on a substrate after API RP 7A1 experiment.....	65

Figure 43. Make-up and break-out versus rotation degree plots for α -ZrP.....	66
Figure 44. Illustration of the role of α -ZrP NPs between sliding surfaces.....	68
Figure 45. Exfoliated layers of α -ZrP [60].....	69
Figure 46. Illustration of the change of the shear line by trapped nanoparticles	69

LIST OF TABLES

	Page
Table 1. Comparison between synthetic oil and mineral oil [24-26]	10
Table 2. Comparison of thickeners [27].....	10
Table 3. Different types of additive in semi-solid lubricants [26].	11
Table 4. Major reasons of a bearing failure [43].....	15
Table 5. Operating costs of replacement of wind turbine parts [44].....	16
Table 6. Characteristics of Super Lube® grease formulation [50]	22
Table 7. Characteristics of Calcium Fluoride Bolt Lube [51].....	22
Table 8. Properties of Inconel A 718 [53].....	23
Table 9. Classification of galling level [51].....	30
Table 10. Comparison of wear depth and width	45
Table 11. Slope of line on the reference grease and the grease with 0.5wt% Y_2O_3	49
Table 12. Comparison of the roughness average	61
Table 13. Comparison of wear depth and width	62
Table 14. Slope of line on the reference grease and the grease with 0.5wt% ZrP	67

CHAPTER I

INTRODUCTION

This chapter provides the basics behind this research and applications. In the first section, the concept of tribology will be briefly explained in terms of friction and wear. Followed by the lubrication part, the types of lubricants will be discussed. Among them, the focus of this research is the semi-liquids lubricant, i.e., grease. Subsequently, the effects of nanomaterials on frictional behavior and wear resistance will be described in terms of additives in lubricants. Finally, the need of lubricants in a wind turbine will be discussed as potential applications.

1. 1. Tribology

The word Tribology was coined in 1966 by the Organization for Economic and Cooperation and Development [1]. Tribology, came from the Greek word “tribos,” is science related to understanding the motion in two interacting surfaces. Topics of tribology consist of friction, lubrication, and wear.

The importance of friction has been studied since early civilizations. Paleontologists discovered that peoples would strike flint or pyrite rocks, or rub sticks together to create sparks or fire [2]. In ancient times, the first lubricant was the olive oil used to move large stones to make pyramids [3] and ancient Sumerians also used grease to lubricate wheel axes [4]. As a science, Leonardo Da Vinci established the law of

friction [5]. He demonstrated that the friction force is proportionate to the object's weight and is independent of geometry with the proposal of many experiments [6].

Among the topics of tribology, wear behavior would be studied in the most recent. When surfaces interact, they inherently generate loss of material or wear caused by friction. To investigate and understand the mechanism of wear, it is a critical issue in machinery which has interacting components [7]. Similar to friction, wearing of material influences the decrease of energy, efficiency, and the lifespan of a material.

The following sections will cover the further understanding of friction and wear mechanisms, as a portion of tribology.

1. 1. 2. Friction

Whenever one solid body slides over another, the resistive force is generated between two surfaces, called the friction force. A friction force can be considered with the deforming of the contacting asperities which results in adhesive contacts [8]. A friction force causes the loss of materials between surfaces interacting with each other. It can be significant issues depending on the situation.

The friction force can be affected by many factors, including geometry, environmental conditions, and material properties. In this research, the analysis of lubricated friction will be observed on different environmental conditions such as high temperature and a load. Lubricated friction can be explained with a lubricating material applied between two moving materials.

Friction is considered to be static and kinetic. Static friction is the force which resists the motion of two bodies which are in contact. A block sitting on an inclined platform can be an example of static friction. Until the force of static friction is overcome, the block will stay on the platform. The amount of static friction would be calculated by various factors such as geometry, the mass, chemical interactions, and electrostatic forces.

Once the static friction is diminished between two objects, the force of kinetic friction would be generated as another resistive force. The value of kinetic friction is typically less than that of static. The relation between static and kinetic friction can be observed in real-life. For example, when one tries to move a large and heavy piece of furniture, once in motion, the force to keep it moving is less than to initiate the motion.

Figure 1 shows the various forces on two interacting surfaces.

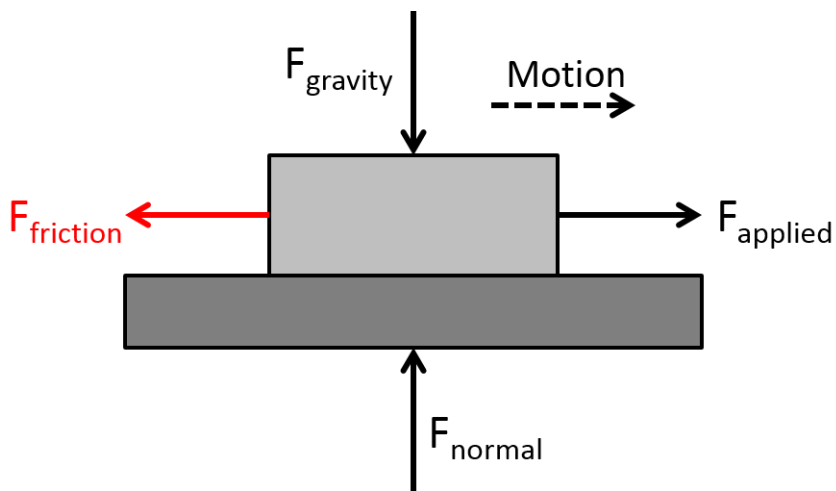


Figure 1. Various forces on two interacting bodies

Other types of friction are consisted of fluidic friction, internal friction, and dry friction. Fluid friction is the force which resists the motion of two bodies between fluids. Internal friction is the resistive force between interacting molecules at the surface. Dry friction refers to the force which resists the motion of two solid objects [9].

The COF can be expressed by the ratio of the frictional force to the applied force as a dimensionless quantity. It will be calculated by below equation:

$$\mu = \frac{f}{N}$$

where f is the resistance force and N is the applied force.

The detailed information for the obtaining the coefficient of friction as experimental methods will be discussed in a later chapter.

1. 1. 3. Wear

Wear is generated between two surfaces interacting with the loss of material, which is related to mechanical and chemical interactions. It can be stimulated by thermal means generated by friction [10]. Typically, the surface characteristics of the material contribute to wear. These can be represented by surface roughness and the wear volume or wear rate.

This research focuses on the wear mechanism on sliding surfaces. A simple analysis of the wear resulting from sliding motion was conducted by Holm and Archard. Holm explained a wear corresponds to atoms being taken away from the surface [11]. Then, Archard described with the explanation of wear caused by clusters of atoms or asperities as opposed to individual atoms [12]. Efforts have been focused on the

mechanisms of wear to ultimately improve machine performance. There are four types of wear, including abrasive, adhesive, fretting, and tribo-chemical wear. First of all, abrasive wear generates when surface asperities are removed due to sliding and abrasion. There are two types of abrasive wear, as depicted in Figure 2. When two interacting materials come into contact during sliding, harder asperities begin to remove softer asperities on the material as shown in Figure 2(a). Once an asperity is removed, it can remain between two surfaces. Such a particle could be abrasive enough to knock out additional debris, as shown in Figure 2(b). When a hard particle remains within the asperities, it gradually causes wear to the softer material. This is called three body abrasive wear.

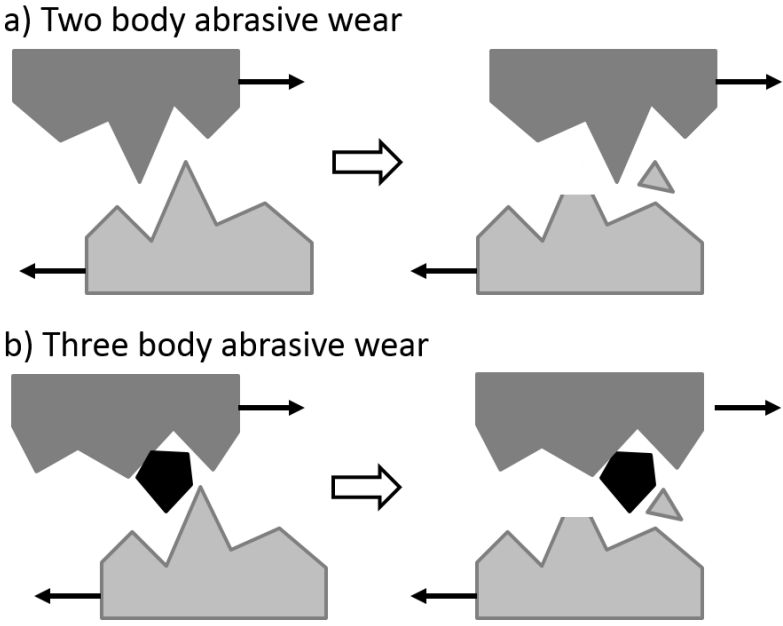


Figure 2. Abrasive removal of one material by another

When hard asperities or particles keep sliding and rolling across the surface, different types of abrasive mechanism can be generated. Those include cutting, fatigue, fracture, and grain pull out [9, 10]. First of all, cutting can be explained when relatively hard particles make grooves on a softer material, called plastic deformation. When the cutting is repeated, fatigue can be generated, as a result of plastic deformation. Fracture occurs with a crack at the surface. It can be described that a hard particle embeds itself in a softer material. Finally, a grain pull out can be generated a grain boundary removed from the surface.

Adhesive wear occurs when the surface of one material adheres to another, as depicted in Figure 3. In this case, wear debris is displaced from the surface of one material and attached to the other material. This mechanism comes from electron transfer with adhesive bonds between the materials at the surface [1, 8].

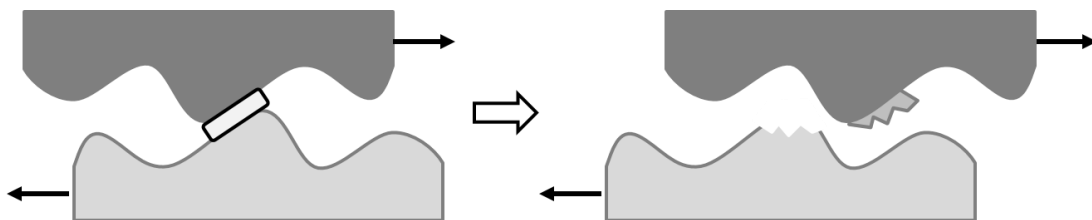


Figure 3. Adhesive removal of one material by another

Fretting occurs under load and in the presence of relative motion by vibration or some other force [13]. In addition, there is a type of corrosive wears caused by the destructive effect of corrosive environment during wear. This is usually identified through oxidation of wear products that are harder than base metals. [11].

Finally, tribo-chemical reaction is the result of chemical reaction during rubbing. Materials in relative motion undergo various chemical reactions due to environmental influences. The reaction generates new compounds. Adsorption is a kind of tribo-chemical mechanisms. It can change surface characteristics and form tribo-layer of new materials [14]. This reaction comes from the presence of humidity in the process [15]. The combination of increased frictional heat and the existence of water vapor can accelerate the development of oxides on the surface. Subsequently, these much harder materials composed of oxides will affect the wear mechanism.

1. 2. Lubrication

Lubrication has been used to reduce friction and wear and prevent the generation of thermal energy between two interacting surfaces. By adding lubricants in a contact area, it can reduce the loss of power and prolong the life of components. In addition, lubricants can serve to remove wear debris and prevent corrosion and rust from two interacting surfaces. Thus, it can reduce the abrasive damage by improving the flow of motion and reducing those particles [16].

Types of lubricants are generally composed of liquid, semi-liquid (grease), solid, gas or any combination of thereof. Each type of lubricants has the pros and cons due to their unique features. For instance, liquid lubricants composed of base oil and additives have low rolling resistance, but need complex sealing device. In case of semi-liquid lubricants which consist of base oil, thickener, and additives, they have relatively long working life span and simple sealing device, but it is used in low rotational speed. Solid

lubricants can be used to high load working condition with low speed, while gas lubricants can be used at high working speed, but it has low load carrying capability [16]. Thus, each type of lubricants should be selected properly depending on the working conditions and the properties of mechanical components.

People consumed 38.2 million tons of lubricants worldwide in 2011 [17]. A large portion of consumption of lubricants comes from automotive applications and other industrial, marine, and metal working applications are also the next consumer of lubricants [18]. Although liquid lubricants dominate the market, semi-liquid and solid lubricants are also used to meet performance requirements.

This research studied grease widely known as a semi-liquid lubricant. Grease is used to lubricate approximately 90 percent of all bearings. But an estimated \$240 billion is lost from an annual break down of bearing only in the U.S., Because of the lack of information and the improperly used lubricants [19]. The improved lubrication of grease will influence on the huge saving of energy and costs in industry.

1. 2. 1. Semi-liquid lubricant

Semi-liquid lubricants and liquid lubricants can be separated by the existence of thickener which can be affected on the viscosity of lubricants. By the presence of thickener, semi-liquid lubricants can be used in different situations with liquid lubricants [20]. For example, semi-liquid lubricants are widely used in many types of gears and ball bearings with relatively high loads and low operating speeds and temperatures.

Semi-liquid lubricant (grease) is composed of base oil (70~90%), thickener (5~25%), and additives (0.5~10%) [21]. Among them, additives are used to serve high performance in severe conditions such as high pressure and temperature. Grease possesses several pros and cons from its functional property. First of all, it can act as a sealant to prevent leakage and to keep out contaminants, because of its consistency. It is easier to contain solid materials than liquid lubricants through its rigidity. However, grease shows poor cooling against the heated surface, due to consistency. It also shows high resistance at start-up than oil. Thus, grease isn't appropriate for low torque or high speed working condition [22]. In order to overcome these obstacles, many researchers have focused on the application of specific additives in grease, such as molybdenum disulfide and graphite with certain mixing techniques.

1. 2. 1. 1. Base oil in grease

Base oil significantly influences the properties of grease such as a working range of temperature, heat resistance, torque, and durability [23]. It can be produced by several types of resources; crude oil, chemical synthesis, and other resources from nature. Base oil derived from different resources can be served on the specific purpose with its advantage and disadvantage, as listed in Table 1. Mineral oil was widely used in lubricants for decades, due to its availability. However, synthetic and natural oil have arisen in many industries since people considered the effects to the environment [24]. When it comes to the reference grease in this research, synthetic oil was considered as the base oil.

Table 1. Comparison between synthetic oil and mineral oil [24-26]

Classification	Type	Advantage	Disadvantage
Synthetic oil	Olefinic	Anti-resinoid Low flow point	Lower lubricity than ester base oil
	Ester	Lubricity Contact resistance	Low anti-resinoid Low anti-rubbery
	Silicon	Oxidation resistance Anti-resinoid	High price Low lubricity
	Fluorine	Oxidation resistance Anti-resinoid	High price
Mineral oil	Paraffin	Lubricity	Low oxidation resistance

1. 2. 1. 2. Thickener in grease

Thickener of 5~20% is used to change the viscosity of grease without affecting the bulk material [21]. There are two types of thickener; soap based thickener and non-soap based thickener [27]. Each thickener shows different properties on its purpose, as explained in Table 2.

Table 2. Comparison of thickeners [27]

Classification	Type	Advantage	Disadvantage
Soap based thickener	Aluminum / Aluminum complex	High temperature stability Oxidation resistance	Stringy Stiffen
	Calcium / Calcium complex	Corrosion resistance High load carrying capability	Relatively low temperature stability
	Lithium / Lithium complex	Long-term and high temperature work stability Corrosion resistance	Relatively low temperature stability
Non-soap based thickener	Polyurea	High temperature stability Oxidation resistance	Low level of compatibility
	Bentonite	High strength	Weakness with high temperature

1. 2. 1. 3. Additives

Additives of 0.5~10% can improve the tribological performance of grease [21].

Additives show the improved chemical characteristics and physical performance of grease. Subsequently, additives can serve to prolong the working life of grease with the decrease of friction, wear, oxidation, and corrosion damage on the applied materials [26].

There are typical additives on its purpose in Table 3. In addition, several types of additives can also improve the stabilization of structures and the oiliness relates to a tendency of grease to wet and adhere to a surface [28], and prevent the scattering of grease and the adhesion of debris [29].

Table 3. Different types of additive in semi-solid lubricants [26].

Additive type	Compound	Function
Extreme pressure / anti-wear	Sulfurized olefins Chlorinated paraffin Metal soaps, including lead Solid additives	Increase load carrying capability Reduce three body wear
Anti-corrosion	Carboxylic acids Fatty amines Metal sulfonates	Form a mono-molecular film or layer
Anti-oxidant	Hindered phenols Aromatic amines Metal dialkyldithiophosphates	Formation of surface film or layer
Lubricity and adherence	Fatty amides, fatty acids, partial esters, polymeric esters Animal and vegetable fatty oil	Maintaining a physical boundary between contacting surfaces
Solid particles	Molybdenum disulfide, Graphite, Boron nitride, Zinc oxide	Thickener, increase load carrying capability

1.2. 2.Nanomaterials as additives in lubricant

Reports have been found in using novel nanomaterials to improve tribological performance. Nanomaterials could be used as lubricants or lubricant additives based on their size, shape, and structure [30].

The first benefit of nanomaterials comes from their nano-size [31]. As depicted in Figure 4, the nanomaterials show higher surface area-to-volume ratio than conventional materials [32]. The nanomaterials, which have high surface area-to-volume ratio, can undergo the faster chemical reaction than the conventional materials. This is because of the high surface energy and the driving force to accelerate thermodynamic process [33]. For example, the nanoparticles can burn at lower temperature than the bulk powder. Thus, rocket uses metal nanopowders as its propellants and explosives [34].

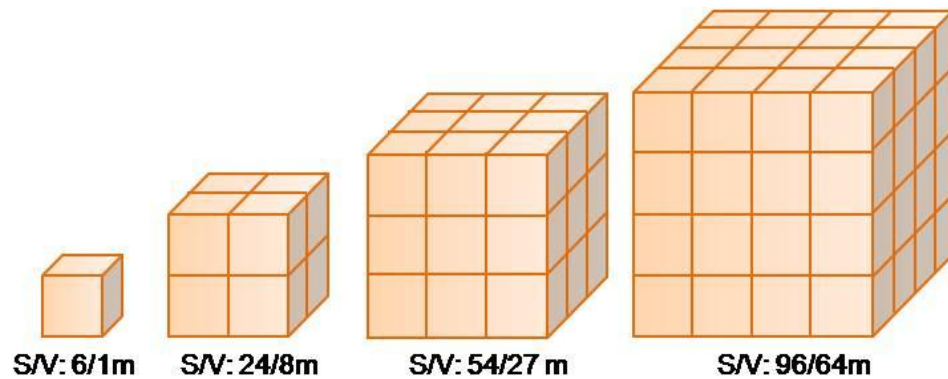


Figure 4. Comparison of surface area-volume ratio according to size [35]

The shape of nanoparticles is an important parameter that can be used in lubricant additives. It is directly related to high load-bearing capability of a lubricant

[36]. For example, under an applied load, nanosheet experiences the least pressure through a planar contact, while the pressure is focused on the small portion of nanosphere due to a point contact, as described in Figure 5 [34]. As a result, nanosheets can endure the larger pressure than nanospheres on the same load carrying capability.

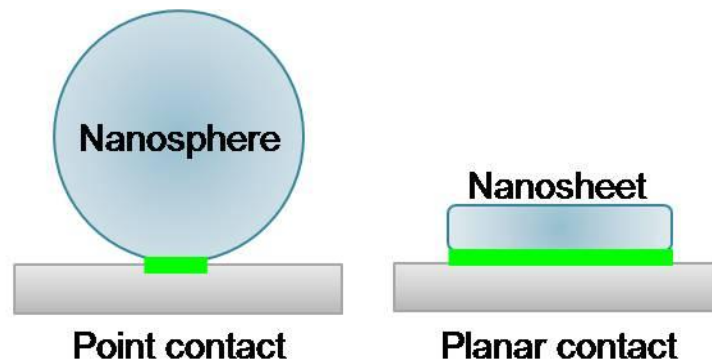


Figure 5. Effect of nanoparticle shape [34]

Finally, the inter-atomic structure influences their mechanical properties and tribological behavior as well. The effect of nanostructure comes from inorganic nanoparticles of layered compounds with a hollow polyhedral structure like MoS_2 [34, 37]. This structure allows rolling and sliding between two surfaces and covering the mating surfaces when they break down and experience material transfer [37, 38]. This effect attributes to reducing friction by forming a physical film on the surface [39].

1. 3. Potential application of the enhanced lubricant in a wind turbine

Friction and wear have been major problems in various industries that can cause additional costs and time on replacements of failed or expired parts in a

machine[40]. The application of adequate and/or improved lubricants can be solutions from the problems[41]. In particular, the importance of tribological improvements is directly related to saving energy and costs in a wind turbine. For the potential applications of this research, the uses of lubricant in the wind turbine will be covered with more specific information in the next section.

1. 3. 1. Necessity of the enhanced lubricants in a wind turbine

A wind turbine which has seen rapid development during the past few years can be determined its capacity by tribological practices. Proper lubrication during working is a main factor to ensure the required operating times and the efficiency. There are several reasons that explain why wind turbine lubrication is critical. First of all, a wind turbine operates in the circumstance with 300 feet in the air, varying speeds and intermittent usage, a high amount of vibration, and extreme working temperature, especially cold. It is also open to the environment such as dirt, dust, and water. In addition, a wind turbine is composed of various mechanical parts, including 4 different bearings, 2 different drives, and 3 different gear boxes [42]. Each component is required different lubricant types due to their operation system. As a result, the wind turbine has been required not only multi-functional lubricants, but also highly developed lubricants to reduce energy and cost losses and span the service life of a turbine.

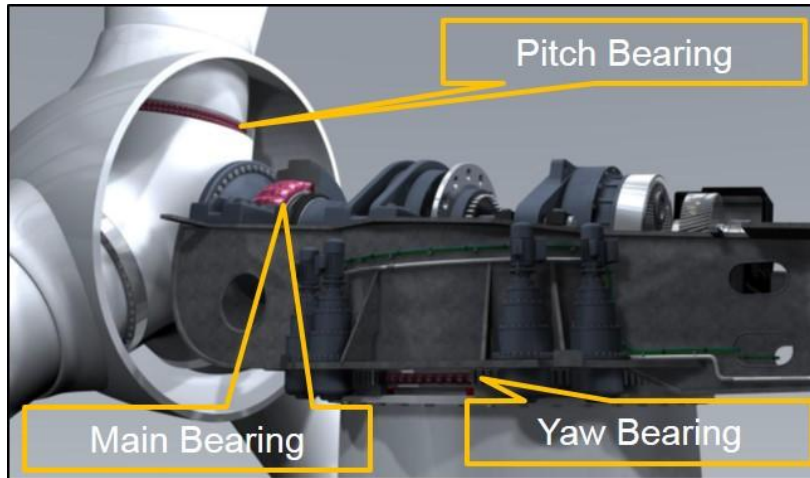


Figure 6. Grease is used at three points in a wind turbine [42]

Figure 6 shows three different bearings which use grease as a lubricant in a wind turbine. Although a working lifespan of bearings was estimated 20years without failure, it has been always failed before a desired service life. Moreover, these failures even happened less than 5years [41]. There are several reasons for bearing failures, but improper lubrication accounts for the largest portion of reason, as shown in Table 4. In order to reach the maximum service life of a wind turbine, a lubricant properly protects the bearing against friction, wear and corrosion, and helps sealing out contaminations [43].

Table 4. Major reasons of a bearing failure [43]

Classification	Potential improvement
Improper lubrication	40~50%
Improper mounting	25~30%
Reaching the nature fatigue limit	< 10%
Other causes	20%

1. 3. 2. Potential savings with lubrication improvement in a wind turbine

The importance of lubricant in a wind turbine can be emphasized in terms of the costs for the replacement of mechanical parts either failure or expired. The replacement costs can be divided into the unplanned and planned operating costs of a wind turbine, as shown in Table 5. The point is that the unplanned costs are much higher than the planned costs, which implies that the sudden failure of mechanical parts requires a significant cost.

Table 5. Operating costs of replacement of wind turbine parts [44]

Operator	Number of turbines	Failure parts	Costs of unplanned replacements(€)	Costs of planned replacements(€)
enviaM	15	3 gear boxes	531,000	132,700
e.disnatur	130	12 gear boxes 40 generator bearings	6,056,000	1,514,000
Juwi	59	20 gear boxes 1 generator bearing 1 main bearing	3,684,600	921,100

Malfunction of a small component in a wind turbine could be fixed with small amounts of replacement costs, but the replacement could be magnified to the change of gear box or generator even a wind turbine itself with huge costs and time. When it comes to the total cost for a replacement component in a wind turbine, materials and labor costs should be included. For example, the costs of changing 2 bearings were estimated US (\$) 5280, including the power not produced during shutdown, the replacement of 2 bearings, and mechanics. However, by using the high performance lubricant, the wind turbine can

improve the efficiency and the output, as well as prevent the malfunction and failure of components. By comparison, the application of high performance lubricant can save US (\$) 15,659.40 than that of standard lubricant during 20 years lifetime [44]. The development of better lubricants is the key to save the unnecessary cost and time in wind power plants and other machinery industry as well.

CHAPTER II

MOTIVATION AND OBJECTIVES

As discussed in the previous chapter, lubricants are very important in a wind turbine. However, the improper and/or poor lubricants cause the failure of a wind turbine before reaching its designed service life. The purpose of this research is to develop novel nanomaterials as additives in grease under the conditions similar in bearings in a wind turbine. The conditions to be examined will be included pressure, speed, and temperature. Commercial lubricants are used as reference.

This research will focus on tribological performance of yttrium oxide and zirconium phosphate as additives in grease. These include friction reduction, anti-wear, and extreme pressure endurance.

The main objectives of this research are to:

1. obtain understanding in tribological performances of yttrium oxide and zirconium phosphate as nanoadditives,
2. determine the feasibility using such nanoparticles in wind turbine applications,
3. understand the mechanisms of the same on lubrication of grease

Overall, this research will reveal the effects of nanoparticles with unique shape and structure on lubrication and obtain new understanding in mechanisms of nanoparticles in grease. The findings in this research will be beneficial to the application of lubricants for high performance machinery and to increase their efficiency.

CHAPTER III

EXPERIMENTAL DETAILS

This chapter discusses materials and experimental approaches conducted in this research. It includes materials, tribometer and galling experimentation, and wear analysis. The first part discusses materials used in this research. Materials include Y_2O_3 and ZrP as additives in a grease, reference grease and sample preparations for tests. Then, this chapter will be followed by tribometer and galling test as experimental approaches. Finally, for the observing of the effects of nanoparticles on wear performance of grease, wear analysis was conducted with the characterization of wear surfaces and the evaluation of wear rate. For characterization of wear surfaces, optical microscope, interferometer, and scanning electron microscope were used in this research.

3. 1. Materials

As discussed in Chapter 1, nanoparticles have been widely studied as additives in lubricants. These studies refer to synthesis and preparation of nanoparticles and their tribological behaviors. However, they have been observed the effects of nanoparticles on liquid or solid lubricants. This research focuses on yttrium oxide (Y_2O_3) and zirconium phosphate (ZrP) as additives for the observation of effects on lubrication of grease. As reference greases, Super Lube was used on tribometer tests and Calcium Fluoride Bolt Lube was used on the galling tests. Finally, Inconel A 718 was used as a substrate for the tribological studies.

3. 1. 1. Yttrium Oxide (Y_2O_3)

Yttrium oxide is an air-stable and white solid substance with cubic structure. It is widely used in commercial products such as the red color in TV picture tubes, microwave and magneto-optical applications. It is also investigated as additives in the commercial lubricants for its effects of oxygen active elements on corrosive wear [45]. Yttrium, one gradient of yttrium oxide, is a transition metal with silver color, which is classified as a “rare earth element.” Yttrium oxide can be synthesized via several methods such as cathode electro deposition, gas-phase condensation, precipitation, sol-gel, pyrolysis, solvo-thermal, and hydrothermal synthesis. Among these methods, hydrothermal synthesis is not only the easiest and cleanest, but also controllable technique for the preparation of yttrium oxide. Yttrium oxide nanosheets synthesized by hydrothermal method and show $316.6 \pm 49.4\text{nm}$ in width and $16.1 \pm 0.9\text{nm}$ in thickness, as shown in Figure 7.

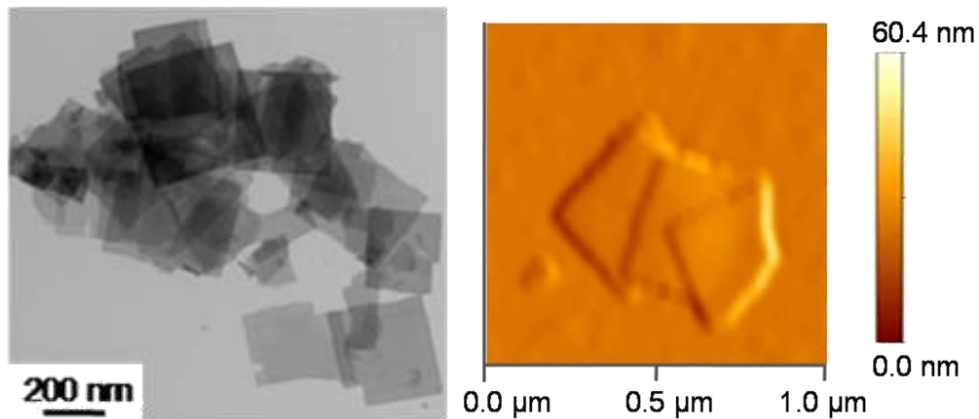


Figure 7. TEM (left) and AFM (right) images of Y_2O_3 NSs [46]

3. 1. 2. Zirconium phosphate (ZrP)

Zirconium phosphate has a lamellar crystal structure with $\alpha\text{-Zr}(\text{HPO}_4)_2 \cdot n\text{H}_2\text{O}$. It has unique properties, including high thermal and chemical stability, ionizing radiation resistance, and ion conductivity in solid state [47]. It also incorporates different types of molecules with different sizes between their layers.

Zirconium phosphate has various phases depending on their inter-laminar spaces and crystalline structure. Among them, the alpha ($\text{Zr}(\text{HPO}_4)_2 \cdot \text{H}_2\text{O}$) and the gamma ($\text{Zr}(\text{PO}_4)(\text{H}_2\text{PO}_4)_2 \cdot \text{H}_2\text{O}$) phases are widely used. In this research, $\alpha\text{-ZrP}$, a synthetic layered compound with well-ordered structure, was studied as an additive in grease [49].

The alpha ($\text{Zr}(\text{HPO}_4)_2 \cdot \text{H}_2\text{O}$) can be synthesized via several methods such as refluxing method, hydrothermal method, and HF method [48]. Among them, hydrothermal method was used in this research for the preparation of $\alpha\text{-ZrP}$. The alpha zirconium phosphate obtained showed a shape of NPs (nanoplatelets) with $600\text{nm} \pm 400\text{nm}$ in width and $19\text{nm} \pm 11\text{nm}$ in height, as shown in Figure 8.

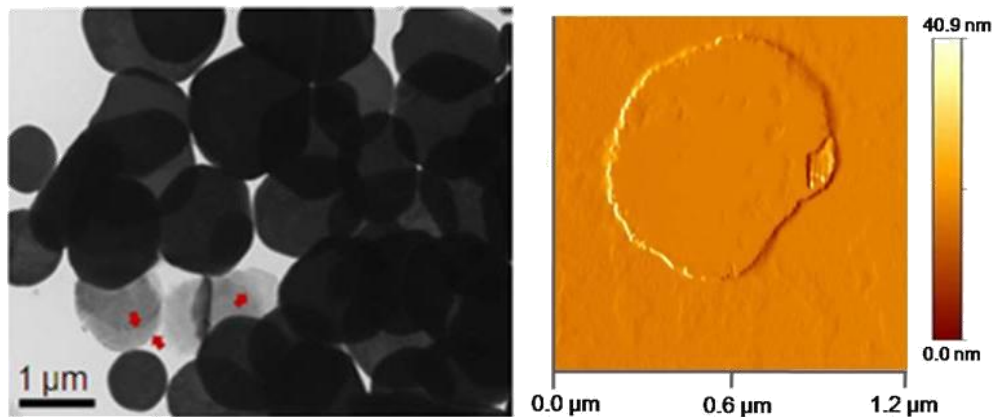


Figure 8. TEM (left) and AFM (right) images of $\alpha\text{-ZrP}$ NPs [49]

3. 1. 3. Reference grease

In order to observe the effects of nanoparticles on various conditions, including a severe condition, reference grease should possess high capability to friction and wear, and it should be widely used in industry for the application of nanoparticles. In this research, Super Lube and Calcium Fluoride Bolt Lube were used on tribometer and galling test. Both have been widely used in industry as bearings, gears, and chains. The detailed information of reference greases are given in Table 6 and Table 7.

Table 6. Characteristics of Super Lube® grease formulation [50]

Component	Wt.(%)	Particle size	Sub-micron
Polyalphaolefin	< 75	Consistency	Worked penetration (60strokes): 265~295
White mineral oil	< 25	Thickener	Fumed silica (5%)
Fumed silica	< 5	Base oil	Polyalphaolefin (PAO) / synthetic
Polytetrafluoroethylene	< 4	Viscosity	At 40°C 75.5cSt
Antioxidant	< 2		At 100°C 8cSt
Polyglycol	< 1		

Table 7. Characteristics of Calcium Fluoride Bolt Lube [51]

Component	Wt.(%)	Particle size	Under 0.1mm
Lithium grease	55	Consistency	Worked penetration (60strokes): 310~340
Calcium fluoride superfine	35	Thickener	Lithium 12-hydroxystearate: 5.5~7.2(%)
Calcium sulfate	8	Base oil	Petroleum / non-synthetic
Van-lube 73	2	Viscosity	At 40°C 115cSt(min) / 170cSt(max)
			At 100°C 9.5cSt(min) / 14.0cSt(max)

3. 1. 4. Substrate material

For the application of enhanced lubricants, a substrate should be considered with compatibility and universality. In that respect, Inconel alloy is one of the most reasonable alloys due to its good tensile, fatigue, creep, and rupture strength. In addition, this alloy has a wide range of applications such as rockets, bearings, and aircraft and various formed turbine engines [50]. There are 8 different types of Inconel alloy according to its composition; Inconel 600, 625, 690, 713, 718, 751, 792, and 939 [52]. In this research, Inconel alloy 718 was used to apply grease and observe the COF and wear resistance on lubrication of grease. Inconel alloy 718 is composed of 50~55% Nickel and Cobalt, 17~21% Chrome, 17% Iron, and 10% other elements [53]. The detailed properties of Inconel A are given in Table 8.

Table 8. Properties of Inconel A 718 [53]

Density	8.19 g/cm ³	Specific heat	435J/kg
Melting point	1260~1336°C	Electrical conductivity	Volumetric, 1.7% IACS at 21°C
Magnetic permeability	1.0011 at RT	Coefficient of thermal expansion	14.0µm/mK at 538°C 15.8µm/mK at 871°C

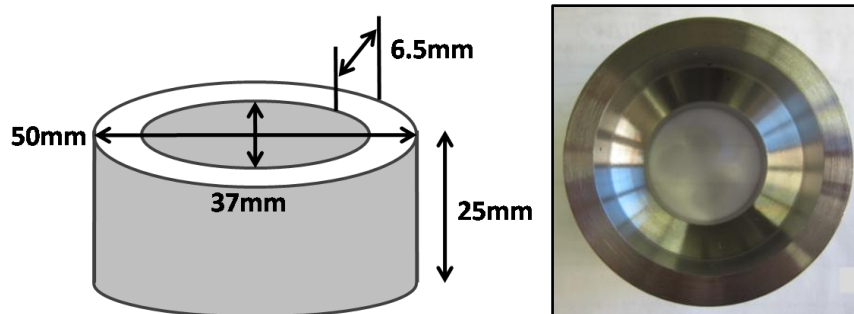


Figure 9. Diagram of Inconel alloy 718 used for tribological test

3. 1. 5. Sample preparation

In order to ensure the effects of nanoparticles, they should be uniformly dispersed in grease with the required concentration. Nanoparticles and grease were stirred for 10minutes in a mortar to blend each other. After stirring, the dispersion of nanoparticles observed by an optical microscope

In order to minimize the effect of the surface roughness on friction, the substrate is polished using 180, 400, and 600 grit sand paper. After polishing, the roughness average of the surface was 20nm on an average of 5 points, as shown in Figure 10. The substrates and ball bearings were washed with acetone and DI water to remove contaminations.

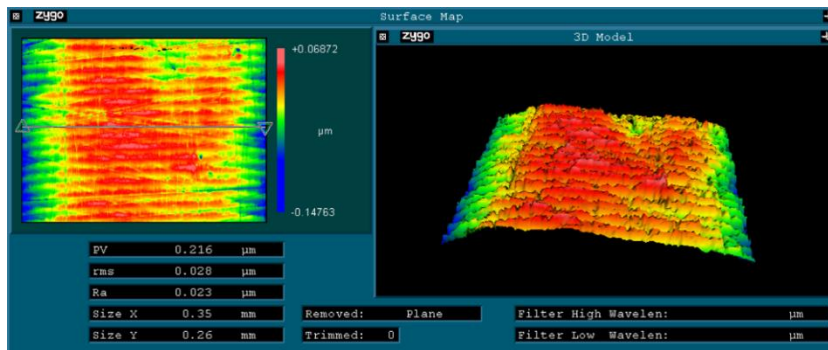


Figure 10. Interferometer results show 20nm of the roughness average for a substrate

3. 2. Tribometer experiments

In order to measure the tribological properties on lubrication of grease, a pin-on-disc tribometer (CSM Instrument) and high temperature tribometer (AMT, Inc.) were

used for friction and wear tests in this research. The first one was used to measure the COF and wear resistance at room temperature. The latter one was prepared to measure the COF at high temperature. They are widely used for measuring the frictional behavior such as lubricating and self-lubricating systems.

3. 2. 1. Pin-on-disc tribometer experiment

A tribological experiment was carried out to observe friction and wear behavior at room temperature. The set-up is shown in Figure 11. It is consisted of a pin, a ball bearing with 7mm diameter (D521000), a measurement arm (sensor), a disc with spindle motor, and a computer. It can be set up with two different modes; the rotating test mode and the reciprocating linear test mode. Typically, the rotating test mode is used on the measurement of COF and the reciprocating linear test mode is used on the observation of wear.

The COF was measured against applied loads, speeds, and time. The range of loads is from 1N to 10N and that of speeds is from 0.1cm/s to 6cm/s. The distance is automatically calculated by applied speeds and a rotating time. In this research, 5 different loads and speeds were input to observe a frictional behavior on different conditions. Applied loads include 1N, 3N, 5N, 7N, and 10N, and rotating speeds were 1cm/s, 2cm/s, 3.5cm/s, 4.5cm/s, and 6cm/s. The applied loads and speeds were considered with the working condition of a wind turbine. In order to develop the wear track used for the observation of wear resistance, 5N loads and 3cm/s speed were set up on tribometer test for 2hours. The linear graph of COF was displayed a computer with a

Tribo X program during the test in real-time. All data can be extracted and saved after the test for further analysis. The average of the COF was obtained since the COF didn't get to see any increase or decrease.

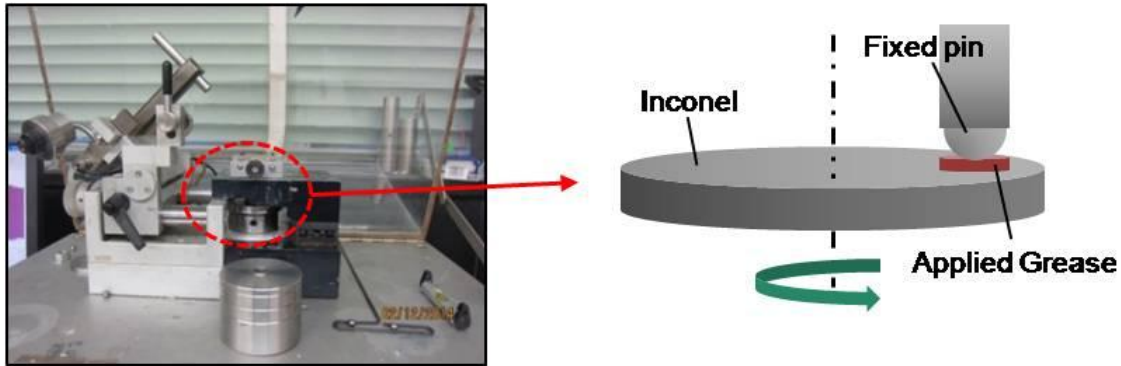


Figure 11. Pin-on-disc tribometer (CSM Instrument)

The tribometer gathers the data from a piezoelectric signal developed between mating surfaces. The contact area between a ball bearing and a disc was relatively smaller than the size of nanoparticles added in grease. For ensuring the effects of nanoparticles added in grease, a ball bearing was ground for 30minutes to obtain a flat surface rubbing with the substrate. As a result, a wear scar which has 141um in diameter was developed on a ball bearing.

3. 2. 2. High temperature tribometer experiment

In order to observe the effects of nanoparticles on lubrication of grease at high temperature, a high temperature tribometer test was done. As described in Figure 12, the setup contains a furnace chamber, spindle motor with a disc, Z-axis shaft with bearing

mount, cooling system, control panel and computer [54]. The furnace chamber can be heated up to 1200°C by electric heating elements with a reflective, gold insulating layer. The Z-axis shaft with load cells measure its deflection along the movement on the disc. The COF measured from the deflection of load cells. The control panel handles all operations and all data including temperature, RPM, the COF, and a load is collected through the control panel and displayed a computer with a Lab View® program.

The applied load was 5 pound and the velocity of spindle disc was set at 100 RPM. The test was conducted for 10minutes, while simultaneously the COF is collected. The ball bearing of 7mm diameter traveled 30mm diameter track on a disc.

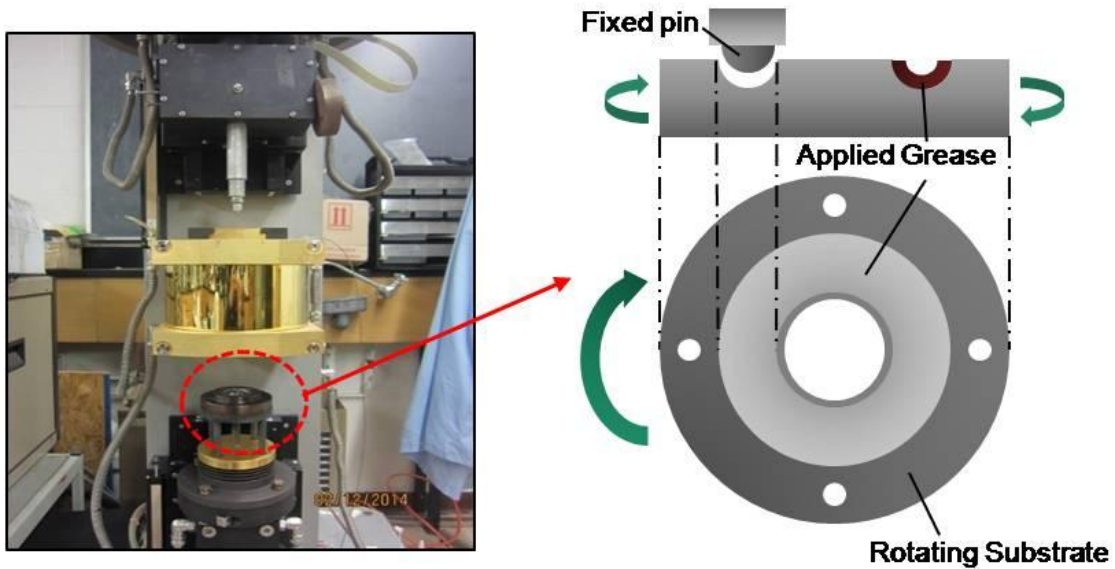


Figure 12. Diagram of a testing configuration for high temperature tribometer

3. 3. Galling experiments

Galling is a form of wear caused by a combination of friction and adhesion between sliding surfaces. In this research, API RP 7A1 machine was used to understand

the effect of nanoparticles on the galling resistance of grease. For comparison, the plot of the torque versus turns was observed during the tests and the friction factor was calculated since all tests were completed.

3. 3. 1. Test procedure

As described in Figure 13, APT RP 7A1 is comprised of computer, a control panel, motor and gearbox, torque transducer and rotation transducer [51]. It can be operated either manually from a control panel or automatically from a computer. When the machine shows a malfunction or doesn't response to a computer signal, it can be controlled manually from the control panel.

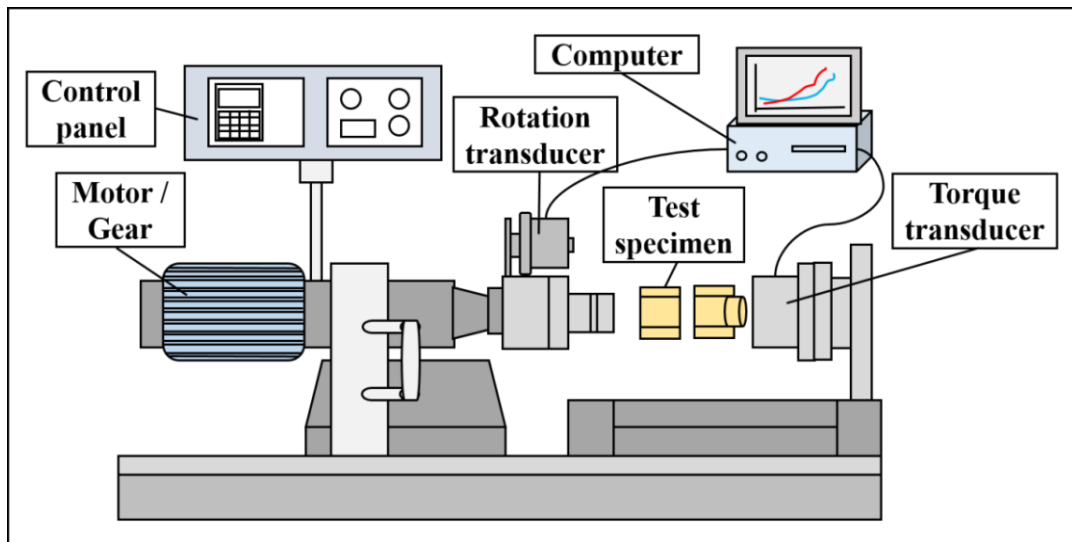


Figure 13. API RP 7A1 used in galling test [51]

As a first step, the appropriate amount of grease is individually applied on two Inconel substrates and these are mounted to cartridge assembly consists of load cells and

hex sockets. Calibrations on two transducers are carried out before conducting each test. Then, motor and gearbox generates torque up to 55,000 pounds with input speeds from 1 to 5RPM. The real-time data on an applied torque and rotation degree is recorded a computer in terms of galling resistance. All data can be used to analyze a make-up process. When the machine approaches the torque near by 55,000 pounds, it stops the operation automatically. Then, it released to an opposite direction of torque. The real-time data is recorded a computer as same as the make-up process. This process calls a break-out process. A complete test consists of three steps as follows:

- 1) Carrying out a first calibration test performed using the reference compound
- 2) Performing a run using the test thread compound
- 3) Carrying out a second calibration test using the reference compound

A minimum of five cycles constitute one test run for either the reference compound or the test thread compound for standard galling tests.

3. 3. 2. Visual inspection

After a test, a specimen should be cleaned with a proper solvent in each process. When a surface of the specimen is observed with naked eyes, if there are any traces of galling, it means that the sample compound doesn't meet the requirements as a grease. Thus, that compound would be rejected and the test would be halted. If there aren't shown any traces of galling, the sample compound would be compared to the reference compound with a data analysis. Table 8 shows a galling level followed by the galling morphology, as described in Table 9 [50].

Table 9. Classification of galling level [51]

Galling level	Description of the galling
1	Clear, little to no light scratches
2	Nicks and scratches, signs of wear
3	Light galling over less than 10% on the circumference
4	Repairable light galling over 10% on the circumference
5	Galling beyond reasonable repair efforts

3. 3. 3. Data analysis

All data from a galling test is automatically recorded a computer, which includes a torque, a load, rotation degree, and a slope of line. From these data, the analysis conducted with the observation of the make-up and the break-out torque versus rotation degree plot and the comparison of a friction factor.

The purpose of the observation of the make-up and the break-out torque versus the rotation degree plot is to verify the existence of galling during the test. If the break-out torque is upper than the make-up torque in certain degree, it means that a galling was developed at that point. Thus, the make-up torque line should be always upper than the break-out torque line to meet the requirements as a lubricant.

In order to compare the galling resistance on lubrication of the reference grease and the grease with nanoparticles, the friction factor calculated by simple formula as shown below should be considered:

$$FF = \frac{2 \cdot S_2}{S_1 + S_3}$$

Where S_1 is the average value of the slope of line on the first 8 runs of a reference compound, S_2 is that of the 8 runs on the test thread compound, S_3 is the average value for the slope of line on the second 8 runs of the reference compound [51]. The purpose of this evaluation is to change the relative value to the modulus value on each compound. The high friction factor means the existence of the high frictional behavior between two mating surfaces, which includes a low galling resistance of a test compound.

3. 4. Wear analysis

In order to characterize the grease and wear morphology, an optical microscope, interferometer, and scanning electron microscopy were used in this research. After the characterization of wear morphology, a wear rate was calculated for comparison of wear performance.

3. 4. 1. Optical microscope

Microscopic images were taken to observe the nanoparticles in grease and the worn surfaces obtained after the tribometer tests. The VHX-600 digital microscope was used at 100, 500, and 1000times magnification. It uses a charge coupled device (CCD) camera to take high resolution images displayed on a monitor in real time. The microscopic images provided the characterization of wear on the specimens and the components in grease after tribometer test. Figure 14 shows the digital optical microscope.



Figure 14. Digital optical microscope (VHX-600)

3. 4. 2. Interferometer

To analyze the surface profile of worn surfaces, interferometer was used to identify a roughness of worn surfaces and wear depth after wear tests. Figure 15 shows the 3D optical surface interferometer (ZYGO NEW VIEW 600). This system uses scanning white light interferometry to image and measure the surface morphology. As a result, it provides the surface roughness data with 2D and 3D images of certain resolution depending on its objective. It has three objectives, including 10, 20, and 50 times magnification. 10 times objective with 0.70 x 0.53 mm of the image size was used in this research. For the accurate data, a vibration isolator was used to eliminate the vibrations.

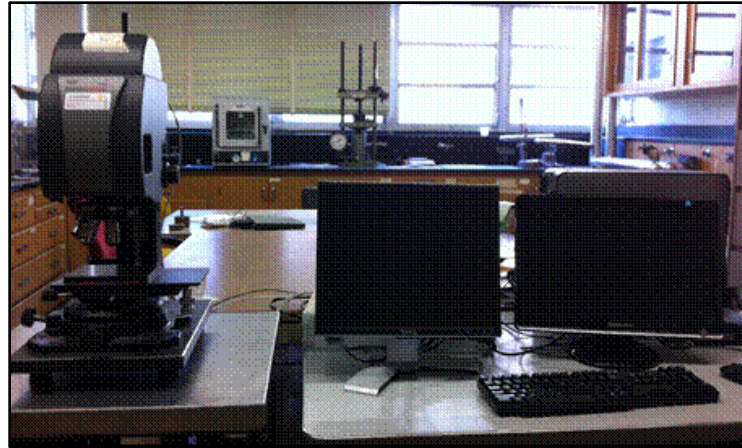


Figure 15. Interferometer (ZYGO NEW VIEW 600)

3. 4. 3. Scanning Electron Microscopy

After tests were completed, scanning electron microscopy (SEM) was used for the further analyzing of the wear tracks on the disc samples. Figure 8 shows the microscope (Quanta 600 field emission scanning electron microscope) used in this research. It contains a Schottky emitter source with a field emission gun and a controllable x-y-z stage. The samples are positioned and manipulated for imaging through the stage. For imaging of the wear track, SEM was set at 1000x magnification and 5kV of the accelerator voltage under a high vacuum.

3. 4. 4. Evaluation of wear rate

In order to evaluate a wear rate, wear volume calculated by wear depth and width. A wear depth can be calculated through an interferometer and a wear width is measured through an optical microscope. As mentioned earlier, an interferometer is suitable for obtaining a wear depth with the surface analysis, including a morphology

and roughness. An optical microscope can be used for the characterization of wear scar and the calculation of wear width. After obtaining a wear depth and width, the wear rate can be calculated by this equation,

$$\text{Wear rate} \left(\frac{\text{mm}^3}{\text{N} \times \text{mm}} \right) = \frac{\text{Wear Depth} \times \text{Wear Width} \times \text{Wear Length}}{\text{Applied Force} \times \text{Sliding distance}}$$

Figure 16 shows the diagram of each parameter to calculate the wear rate.

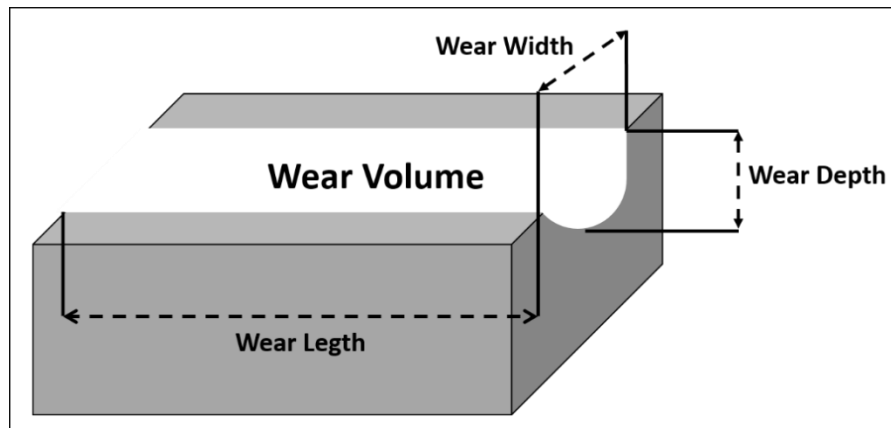


Figure 16. Diagram of parameter to calculate a wear rate

CHAPTER IV

EFFECTS OF Y_2O_3 AS ADDITIVES ON LUBRICATION OF GREASE

This chapter discusses the influence of Y_2O_3 nanosheets (NSs) on lubrication while added in grease. In the first section, the effects of Y_2O_3 NSs on the frictional behavior of grease will be discussed. Topics include the critical concentration of NSs, and the comparison of the coefficient of friction (CoF) as a function of applied loads, speeds, and temperature. In the second section, the effects on wear will be described in terms of morphology and wear rate. Subsequently, the galling resistance will be examined. Finally, the mechanisms of Y_2O_3 additives on lubrication of grease will discuss in the respect of the shape of nanoparticles.

4. 1. Effects on frictional behavior

In order to observe the frictional behavior of the grease with Y_2O_3 , the coefficient of friction (CoF) was determined with tribometer experiments. The CoF of the grease containing Y_2O_3 significantly decreased either at room temperature or high temperature. The change in the CoF over time was observed at room temperature and high temperature by tribometer experiments. All tribometer experiments were carried out when the CoF didn't experience any increase or decrease. Statistical analysis was performed to observe whether there was any difference between the reference grease and the grease with Y_2O_3 .

4. 1. 1. Dispersion of Y_2O_3 in grease

Uniformly distributed nanoparticles in grease are important for consistent performance. Optical microscope was used to observe the dispersion of Y_2O_3 NSs in grease. Figure 17 shows the optical microscope images of the grease with (left) and without (right) Y_2O_3 . The left figure indicates the reference grease and the right figure is the image of the grease with 0.5wt% Y_2O_3 . In the case of the grease with 0.5wt% Y_2O_3 , there are many particles distributed uniformly. The proper dispersion of Y_2O_3 is a critical factor to ensure the effect of NSs on lubrication of grease.

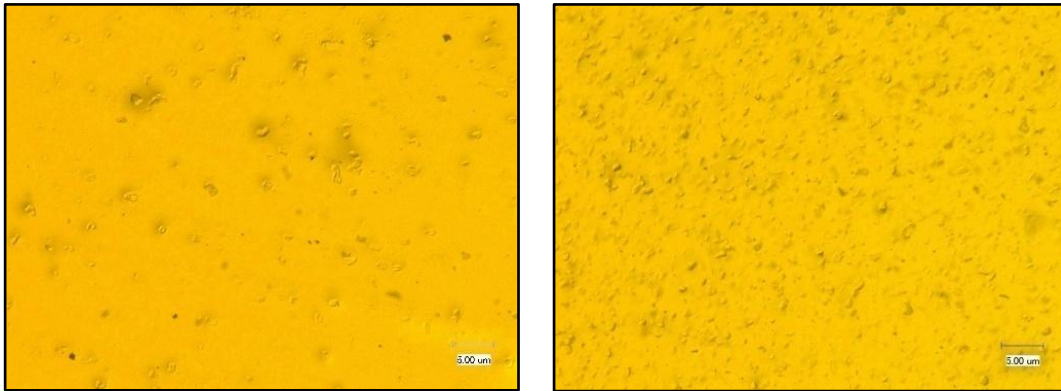


Figure 17. OM images of the reference grease (left) and Y_2O_3 (right) at 1000x

4. 1. 2. Effects on concentration

The concentration of additives in grease should be considered because grease usually consists of 0.5%~10% additives [21]. The CoF of 0.1wt%, 0.5wt%, and 1.0wt% Y_2O_3 NSs in grease was compared to observe the effect of concentration. As shown in Figure 18, the CoF was decreased with 0.5wt% Y_2O_3 NSs. However, the addition of 0.1wt% of Y_2O_3 NSs in grease didn't show any change in the CoF. The addition of 0.5wt% and

1.0wt% of Y_2O_3 NSs in grease showed 5.35% and 7.14% decrease of the CoF, respectively. This result shows that Y_2O_3 NSs are acceptable as additives in grease because the small amounts of Y_2O_3 NSs (less than 1.0wt%) were enough to improve the frictional behavior of grease.

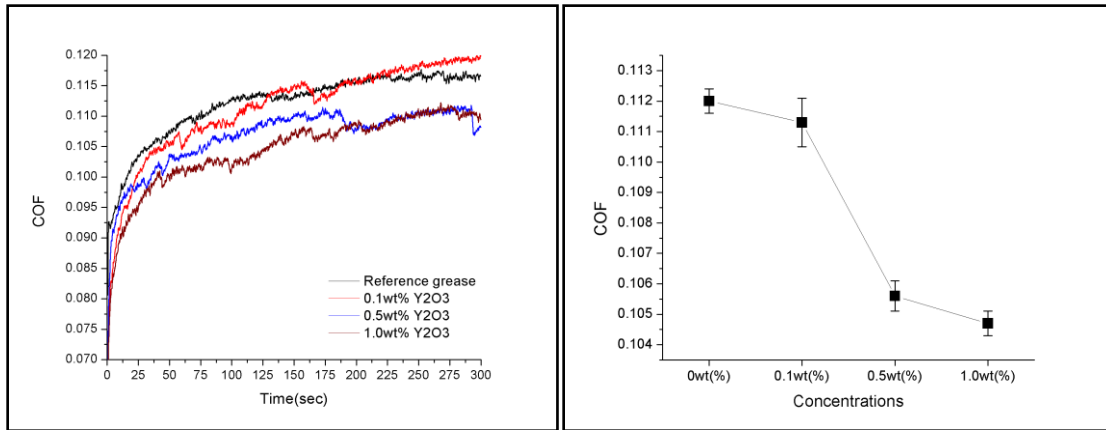


Figure 18. Comparison of the CoF from different concentrations

4. 1. 3. Effects of Y_2O_3 on frictional behavior of grease at room temperature

For the comprehension of frictional behavior with Y_2O_3 NSs, a pin-on-disc tribometer experiment was conducted at room temperature with the different loads and rotating speeds. The different friction responses were observed depending on the applied loads and speeds.

Figure 19 shows the comparison of the CoF under different loads. The CoF of the grease with 0.5wt% Y_2O_3 NSs obviously decreased in all loads, when it compared to the reference grease. The decrease rates of the CoF between two samples are 8.4% under 1N, 24.4% under 3N, 11.9% under 5N, 7.2% under 7N, and 4.9% under 10N. On an average,

the CoF showed 11.3% decrease with the addition of Y_2O_3 NSs in grease. This result can be explained with the rotating and sliding of Y_2O_3 NSs between two surfaces. The rotating and sliding motions contributed to the low shear stress and formed a thin physical film. Further analysis will be covered in the mechanism section.

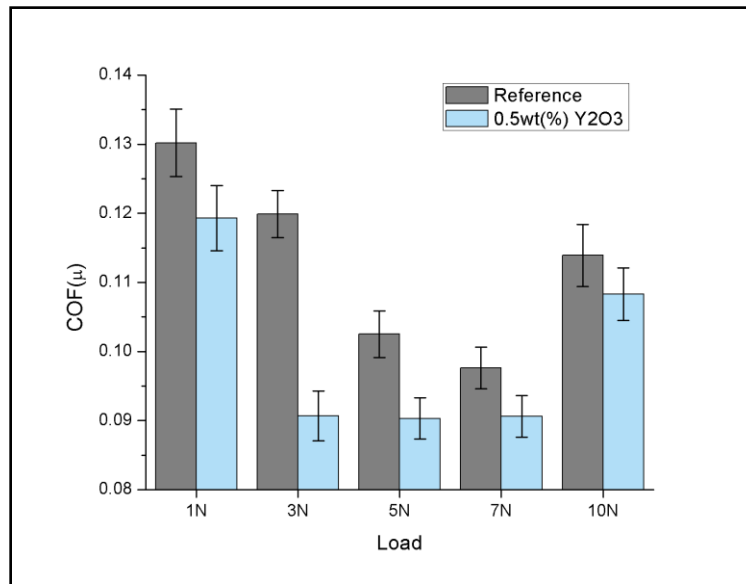


Figure 19. Comparison of the CoF under different loads

Figure 20 shows the comparison of the CoF at different speeds. The significant decrease in CoF was only observed at low rotating speeds (<150RPM). The decrease rates of the CoF between the grease with and without Y_2O_3 NSs are 29.5% at 50RPM, 16.6% at 100RPM, 3.7% at 150RPM, 9.7% at 300RPM, and 6.7% at 400RPM respectively. The results show that the rotating and sliding effects of Y_2O_3 NSs enable at all rotating speeds.

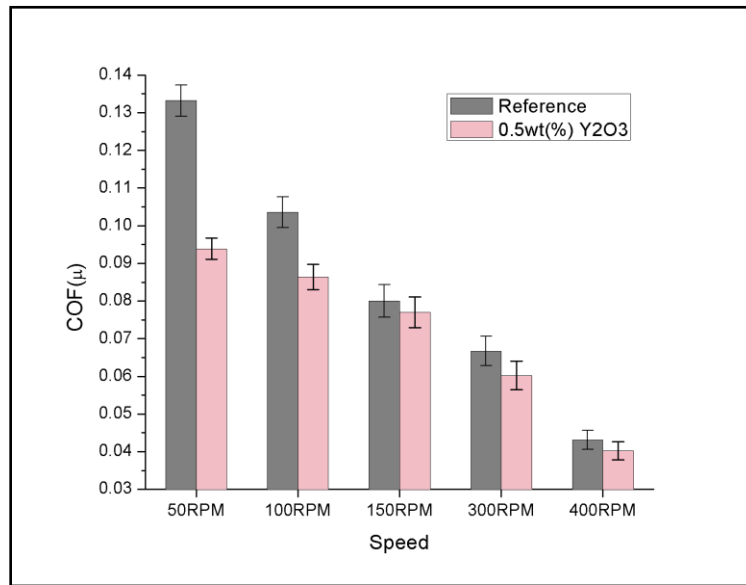


Figure 20. Comparison of the CoF at different rotating speeds

In the frictional performance on lubrication of grease, the addition of Y₂O₃ NSs shows the decrease of the CoF under different loads and at rotating speeds. These results can be explained with the opportunity for the decrease of friction with rotating and sliding of Y₂O₃ NSs.

4. 1. 4. Effects on frictional behavior at high temperature

The working temperature of a wind turbine is estimated from -20°F (-28.89°C) to 300°F (148°C) depending on its service places such as sea and desert [44]. For the potential application in a wind turbine, the addition of Y₂O₃ should show the enhanced performance on lubrication of grease at elevated temperatures.

It was observed that the CoF at high temperature for the comparison of frictional behavior of grease. Figure 21 shows the CoF of the reference grease and the grease with 0.5wt% Y_2O_3 NSs according to the elevated temperature. The grease with 0.5wt% Y_2O_3 NSs consistently shows the lower CoF than the reference grease at 25°C, 50°C, 100°C, 150°C, and 200°C, respectively. The average decrease in CoF shows 13.1% with the addition of 0.5wt% Y_2O_3 in grease. Two samples simultaneously show the decrease in CoF with the increased temperature. This phenomenon can be explained with the decreased viscosity of grease at a high temperature [46]. This indicates that Y_2O_3 NSs are thermally stable at high temperature. The thermal stability provided the opportunity for Y_2O_3 NSs to be able to rotate and slide in the contact area. Similar to the experiment at room temperature, this phenomenon also reduced friction at high temperature.

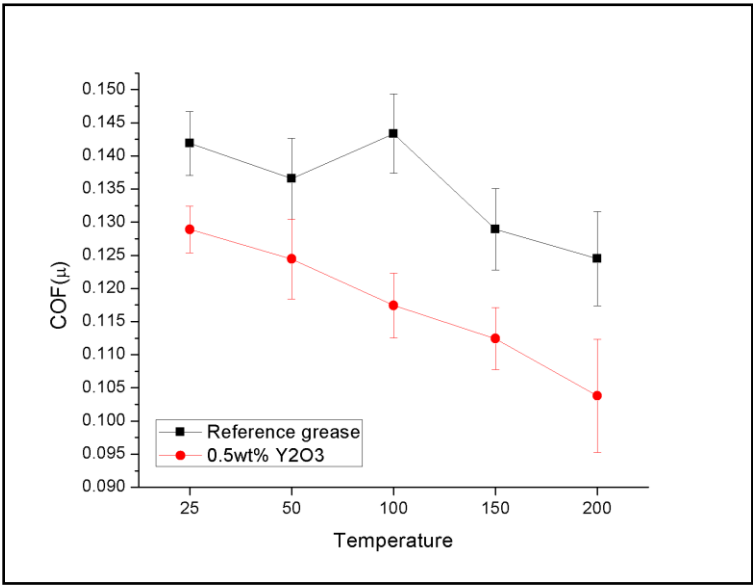


Figure 21. Comparison of the CoF with increased temperature

4. 2. Effects on wear

This section discusses about the wear resistance of grease that was significantly increased with the addition of Y_2O_3 NSs. In this section we analyze the wear scar and the wear track of worn surfaces after pin-on-disc tribometer experiments. The morphology of the wear scar and the wear track was characterized by optical microscope, interferometer and SEM.

4. 2. 1. Analysis of wear scar and wear track on worn surfaces

Figure 22 shows optical microscope (OM) images of the wear scar on ball bearings used in a pin-on-disc tribometer. The left figure clearly shows a larger area of worn scar than the right figure as marked with red circles. The reference grease developed a severe wear scar on the ball bearing, while the addition of Y_2O_3 NSs in grease protected the ball bearing from developing a severe wear scar.

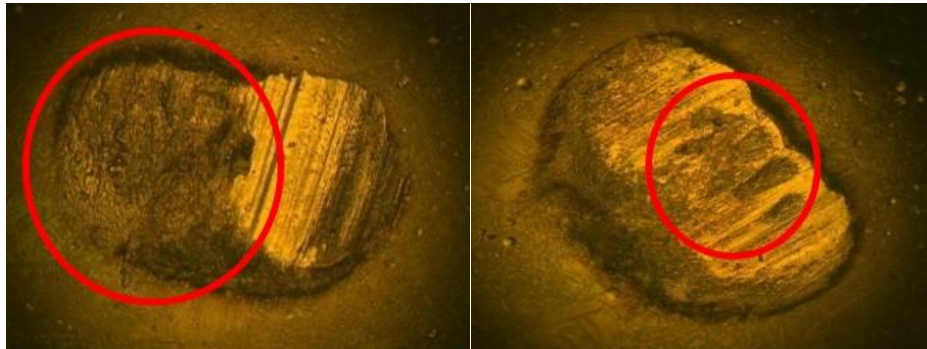


Figure 22. OM images of the wear scar of the reference grease (left) and Y_2O_3 (right)

Figure 23 shows the wear tracks of the reference grease and the grease with 0.5wt% Y_2O_3 NSs after a pin-on-disc tribometer experiment for 2hours. In optical images, the dark color portion indicates the deformation of surfaces. When compared two images, the wear track of 0.5wt% Y_2O_3 NSs shows slightly the smaller dark portion than the reference grease. This means that the addition of Y_2O_3 NSs protected the surface from the deformation caused by friction and heat.

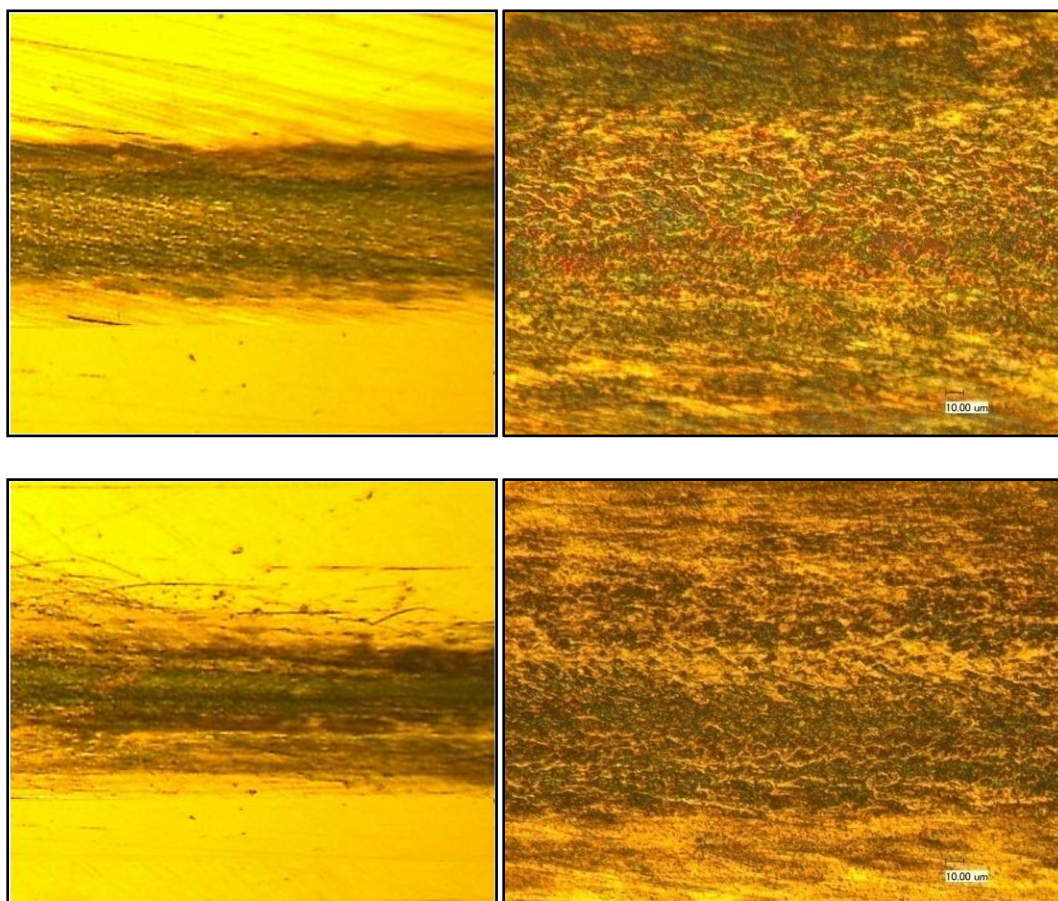


Figure 23. OM images of wear track of the reference grease (up) and Y_2O_3 (down)

Figure 24 shows the 2D analysis images of a wear track using an interferometer. It clearly shows the narrow wear track in the right figure. A wear depth used for the calculation of wear volume was obtained from this 2D analysis. The detailed information of wear depth will be covered in the wear rate section.

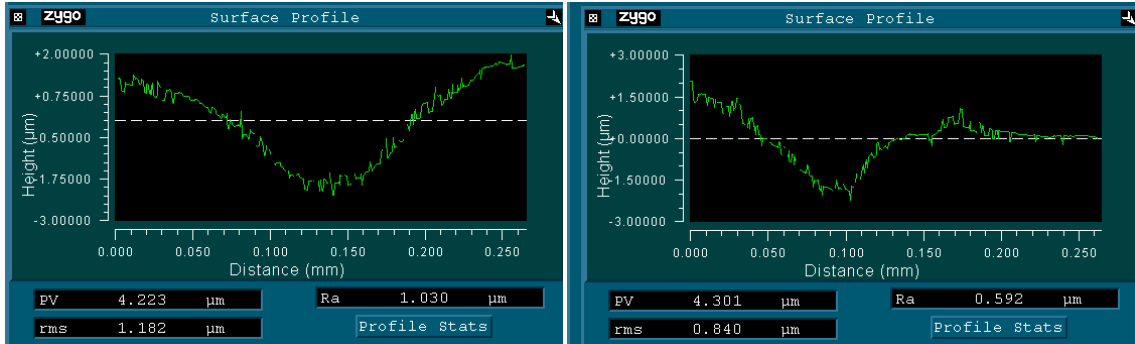


Figure 24. Interferometer results on the reference grease (left) and Y₂O₃ (right)

4. 2. 2. Analysis of roughness on worn surface

For the analysis of the morphology of wear surface, including the roughness and the wear depth within a wear track, an interferometer was used in this research. Figure 25 shows the interferometer results for analyzing the morphology of wear track with 2D and 3D images. The grease with 0.5wt% Y₂O₃ clearly shows a narrow and smooth surface within the wear track. In all data from the interferometer results, including a peak to valley and a roughness average, the grease with 0.5wt% Y₂O₃ was improved than the reference grease. In a roughness average data, the results show 1.094μm in the reference grease and 0.786μm in grease with 0.5wt% Y₂O₃. The addition of Y₂O₃ allowed decreasing the irregularity of sliding surface.

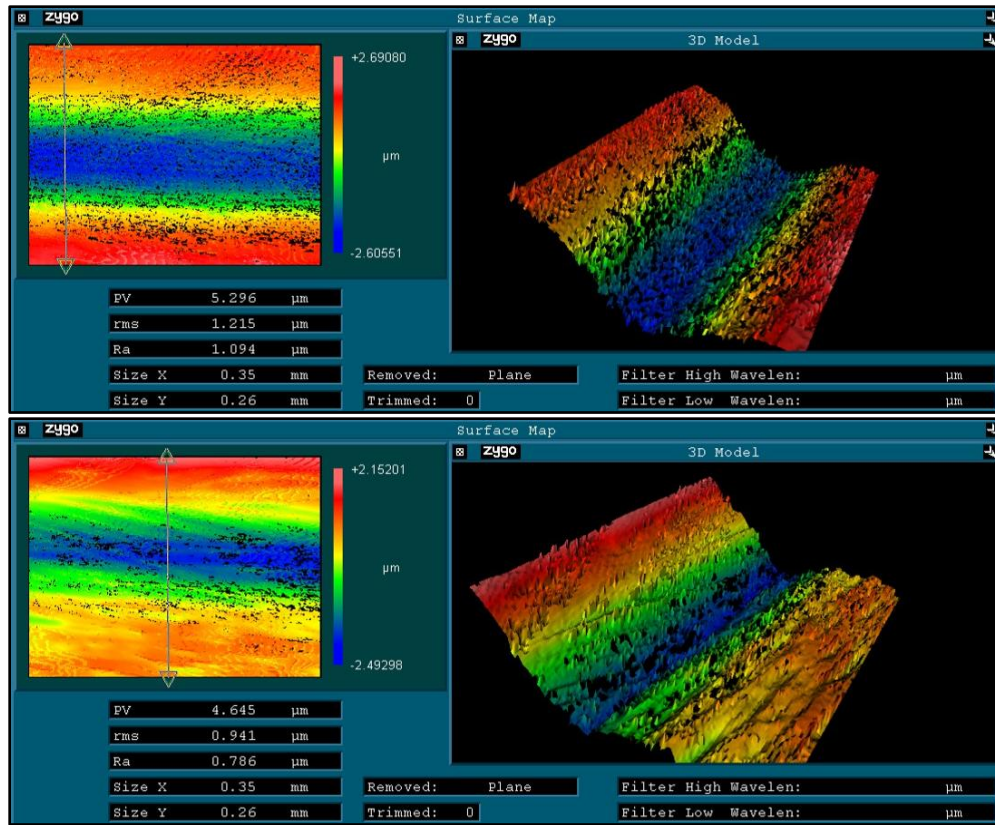


Figure 25. Interferometer results on the grease without (up) and with Y_2O_3 (down)

4. 2. 3. Comparison of wear rate

From the optical microscope and interferometer analysis, a wear depth and width were obtained to measure the wear rate. Table 10 shows the result of wear depth and width on the reference grease and the grease with 0.5wt% Y_2O_3 . The averages of wear depth and width show 2.016 μm and 263.41 μm in the reference grease and 1.967 μm and 260.36 μm in the grease with 0.5wt% Y_2O_3 , respectively. The result indicates that the wear depth and width are slightly decreased to 2.4% and 1.2%.

Table 10. Comparison of wear depth and width

No.	Reference Grease(μm)		Grease with 0.5wt.% Y_2O_3 (μm)	
	Wear depth	Wear width	Wear depth	Wear width
1	2.203	268.84	2.195	261.16
2	2.132	273.02	1.831	268.79
3	2.278	270.71	2.131	259.25
4	2.068	248.01	2.023	278.32
5	1.998	280.63	1.638	272.62
6	1.788	257.37	1.857	268.08
7	1.891	247.88	1.977	254.68
8	2.207	249.75	2.184	242.01
9	1.585	274.53	1.851	238.35
Average	2.017	263.41	1.967	260.36

As mentioned in Chapter III, a wear rate can be calculated by a wear volume, an applied load and a sliding distance. As a result of the calculation, the wear rate of the grease with 0.5wt% Y_2O_3 was decreased to 3.6% than that of the reference grease, as shown in Figure 26. This means that the addition of Y_2O_3 NSs didn't show significant increase on the wear resistance of grease.

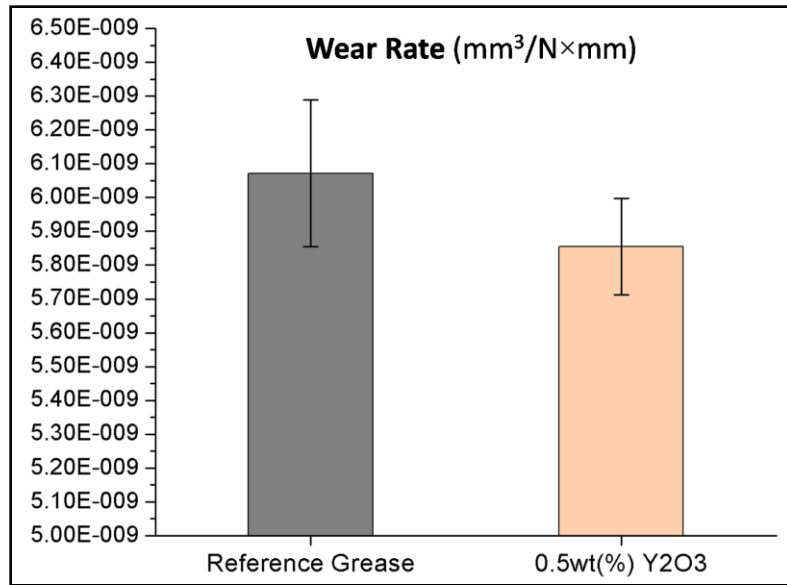


Figure 26. Comparison of wear rate

4. 3. Effects on galling resistance

In terms of galling resistance, the grease shows the reduced frictional behavior and the acceptable galling level with Y₂O₃ under high load. In this research, API RP 7A1 experiment was conducted for the observation on the galling resistance of grease. Once all experiments were completed, visual inspection and data analysis were carried out.

4. 3. 1. Visual inspection

For the visual inspection, the specimen was examined by the naked eye after all tests. As shown in Figure 27, the reference grease and the grease with 0.5wt% Y₂O₃ didn't form any galling traces or scratches between sliding surfaces. All visual inspections met the galling level 1 or 2, as described in Chapter III. It can be explained that the grease with and without 0.5wt% Y₂O₃ meet the requirement as lubricants.

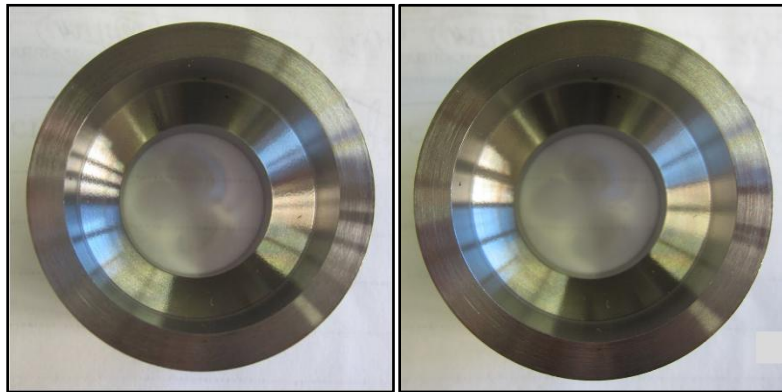


Figure 27. No galling traces on a substrate before (left) and after (right) experiment

4. 3. 1. Data analysis

Data analysis is comprised of the torque versus turns plot analysis and the comparison of friction factor. The make-up torque and the break-out torque versus rotation degrees were plotted to inspect the existence of gall on sliding surfaces during all experiments. As shown in Figure 28, the results of the grease with 0.5wt.% Y_2O_3 show that the make-up torque is clearly upper than the break-out torque in all experiments. Therefore, the grease with 0.5wt% Y_2O_3 performed properly as a lubricant for the galling resistance.

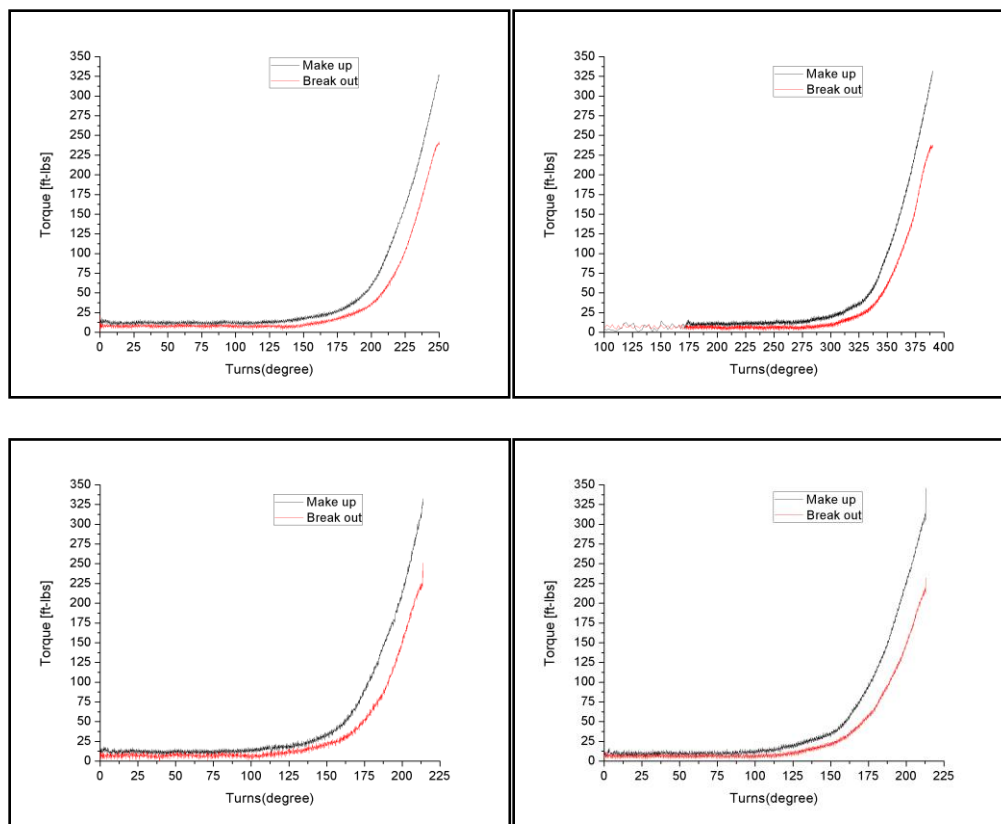


Figure 28. Make-up and break-out versus rotation degree plot for Y_2O_3

A friction factor is used to convert the relative frictional behavior of grease for the absolute evaluation by using the reference compound [51]. As shown in Table 11, the friction factor of the reference grease is 1.261 and that of the grease with 0.5wt% Y_2O_3 NSs is 1.298. In the comparison of the friction factor, the grease with 0.5wt% Y_2O_3 NSs shows the decreased frictional behavior of 10% under high load (up to 55,000pounds). This means that Y_2O_3 didn't remain its crystalline structure under high load. In addition, the broken nanoparticles aggregated. Subsequently, Y_2O_3 couldn't

affect to the frictional behavior of grease. Even the aggregated nanoparticles increased friction between the sliding surfaces.

Table 11. Slope of line on the reference grease and the grease with 0.5wt% Y_2O_3

	1 st reference compound	0.5wt% Y_2O_3	2 nd reference compound	1 st reference compound	Super Lube	2 nd reference compound
1	3.67	4.84	4.42	4.19	4.45	3.97
2	3.64	4.77	3.63	3.93	5.42	3.82
3	3.54	4.79	3.46	4.06	4.5	3.69
4	3.35	4.47	3.51	4.12	4.58	3.48
5	3.42	4.56	3.47	3.87	4.11	3.49
Average	3.524	4.686	3.698	3.63	4.61	3.69
Friction factor	1.298			1.261		

4. 4. Mechanisms of Y_2O_3 NSs on lubrication of grease

The experimental results of this research represent only the reduced friction with the addition of Y_2O_3 in grease. The mechanism can be proposed with the nanosheet shape.

The explanation on the enhanced lubrication of the grease with Y_2O_3 comes from the shape of nanosheets. As depicted in Figure 29, Y_2O_3 NSs could rotate and slide in the contact area. The rotating and sliding motions of nanosheets decreased the direct contact of asperities on the mating surfaces. Subsequently, the cold-welding of asperities which cause the deformation of surface was restrained, and friction was decreased with the low shear stress. In addition, the alignment of Y_2O_3 NSs under an applied pressure reinforced the effect of such behavior [46].

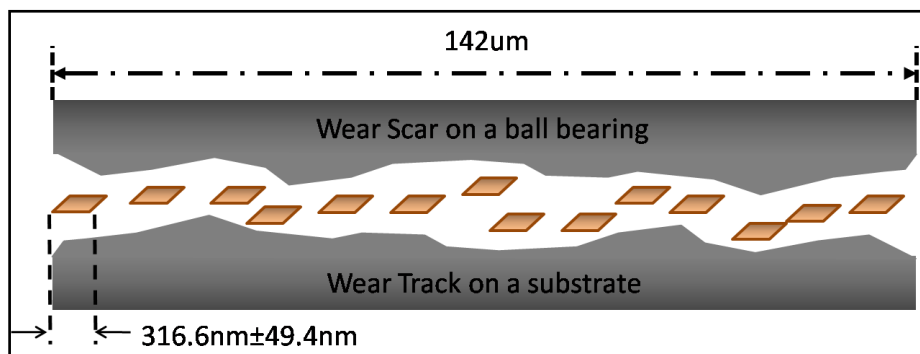


Figure 29. Illustration of the role of Y_2O_3 NSs between sliding surfaces

The nanosheet shape of Y_2O_3 was significantly improved the frictional behavior on lubrication of grease. In addition, the high thermal stability of Y_2O_3 maintained the shape of Y_2O_3 at high temperature.

The effects of Y_2O_3 NSs were discussed on lubrication of grease in this chapter. The next chapter will be covered with the effects of α -ZrP NPs on lubrication of grease, in terms of tribological behavior.

CHAPTER V

EFFECTS OF α -ZrP AS ADDITIVES ON LUBRICATION OF GREASE

This chapter discusses the result of experiments which were conducted on the grease containing α -ZrP nanoplatelets (NPs). In the first section, the effects of α -ZrP NPs on the frictional behavior of grease will be discussed. Topics include the critical concentration of NPs, and the comparison of the coefficient of friction (CoF) as a function of applied loads, speeds, and temperature. In the second section, the effects on wear will be described in terms of morphology and wear rate. Subsequently, the galling resistance will be examined. Finally, the mechanisms of α -ZrP additives on lubrication of grease will be discussed in the respect of the shape and structure of nanoparticles. .

5. 1. Effects on frictional behavior

The CoF of the grease containing α -ZrP significantly decreased either at room temperature or high temperature. The change in the CoF over time was observed at room temperature and high temperature by tribometer experiments. All tribometer experiments were carried out when the CoF didn't experience any increase or decrease. Statistical analysis was performed to observe whether there was any difference between the reference grease and the grease with α -ZrP.

5. 1. 1. Dispersion of α -ZrP in grease

Uniformly distributed nanoparticles in grease are important for consistent performance. Optical microscope was used to observe the dispersion of α -ZrP NPs in

grease. Figure 17 shows the optical microscope images of the grease with (left) and without (right) α -ZrP. The left figure indicates the reference grease and the right figure is the image of the grease with 0.5wt% α -ZrP. In the case of the grease with 0.5wt% α -ZrP, there are many particles distributed uniformly. The proper dispersion of α -ZrP is a critical factor to ensure the effect of NPs on lubrication of grease.

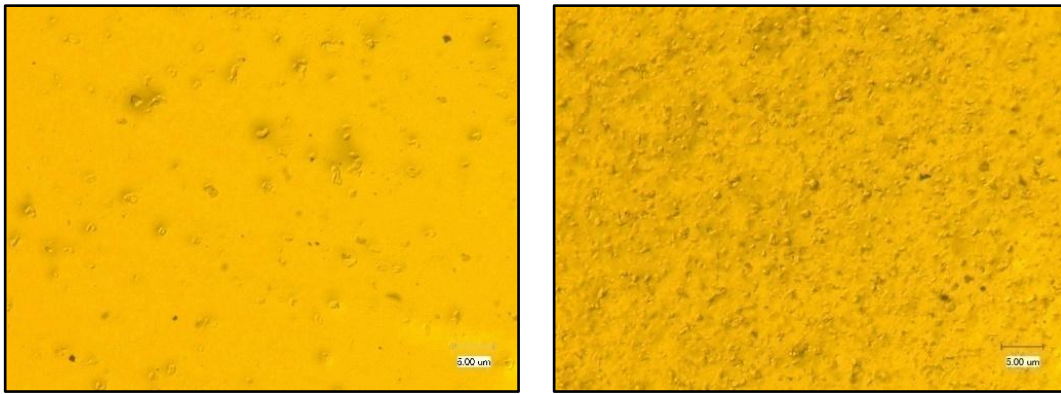


Figure 30. OM images of the reference grease (left) and α -ZrP (right) at 1000x

5. 1. 2. Effects on concentration

The concentration of additives in grease should be considered because grease usually consists of 0.5%~10% additives [21]. The CoF of 0.1wt%, 0.5wt%, and 1.0wt% α -ZrP NPs in grease was compared to observe the effect of concentration. As shown in Figure 18, the CoF was decreased with 0.5wt% of α -ZrP NPs. However, the addition of 0.1wt% of α -ZrP NPs in grease didn't show any change in the CoF. The addition of 0.5wt% and 1.0wt% of α -ZrP NPs in grease showed 5.16% and 5.82% decrease of the CoF, respectively. This result shows that α -ZrP NPs are acceptable as additives in grease

because the small amounts of α -ZrP NPs (less than 1.0 wt%) were enough to improve the frictional behavior of grease.

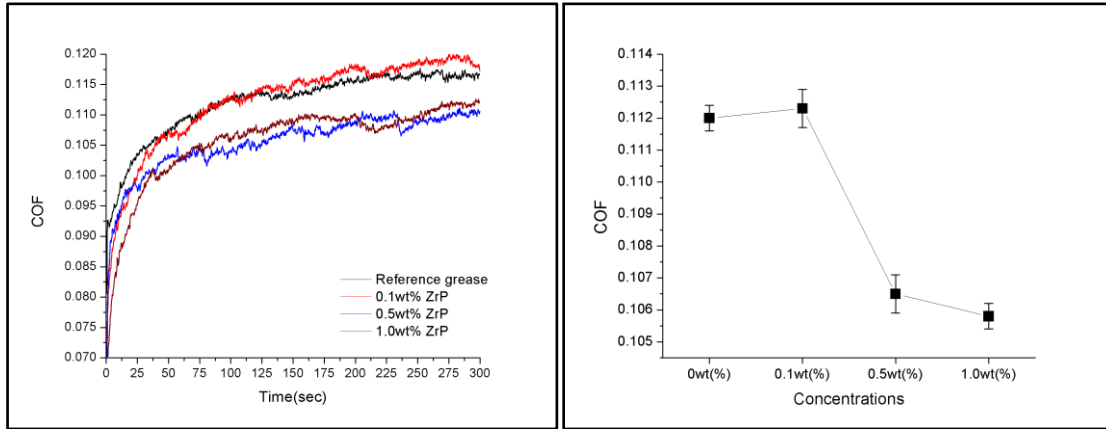


Figure 31. Comparison of the CoF from different concentrations

5. 1. 3. Effects on frictional behavior at room temperature

For the comprehension of frictional behavior with α -ZrP NPs, a pin-on-disc tribometer experiment was conducted at room temperature with the different loads and rotating speeds. The different friction responses were observed depending on the applied loads and speeds.

Figure 19 shows the comparison of the CoF under different loads. The CoF of the grease with 0.5wt% α -ZrP NPs obviously decreased in all loads, when it compared to the reference grease. The decrease rates of the CoF between two samples are 36.7% under 1N, 16.5% under 3N, 16.8% under 5N, 7.3% under 7N, and 11.7% under 10N. On an average, the CoF showed 17.8% decrease with the addition of α -ZrP NPs in grease. This result can be explained with the rotating and sliding of α -ZrP NPs between two surfaces.

The rotating and sliding motions contributed to the low shear stress and formed a thin physical film. Further analysis will be covered in the mechanism of nanoparticles section.

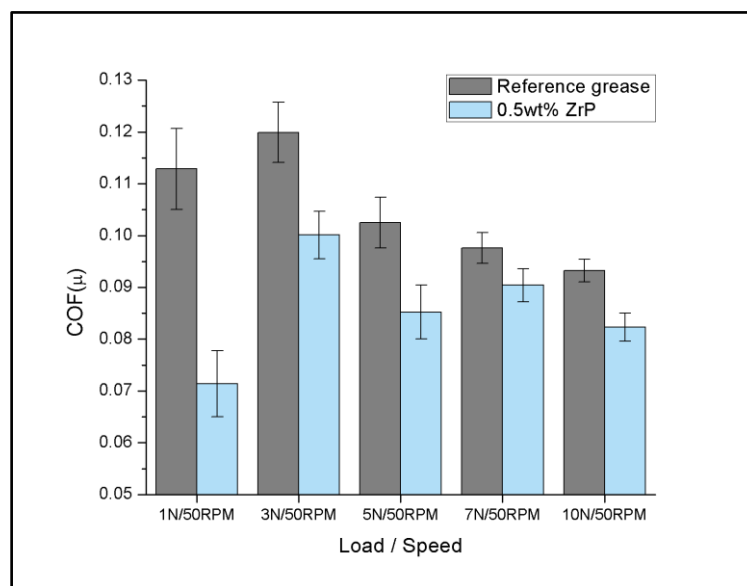


Figure 32. Comparison of the CoF under different loads

Figure 20 shows the comparison of the CoF at different speeds. The significant decrease in CoF was only observed at low rotating speeds ($<150\text{RPM}$). The decrease rates of the CoF between the grease with and without $\alpha\text{-ZrP}$ are 36.7% at 50RPM, 14.4% at 100RPM, and 12.2% at 150RPM, respectively. However, the rates were constant at high speeds (300RPM and 400RPM). The results show that the rotating and sliding effects of $\alpha\text{-ZrP}$ NPs only enable at low rotating speeds (below 300RPM).

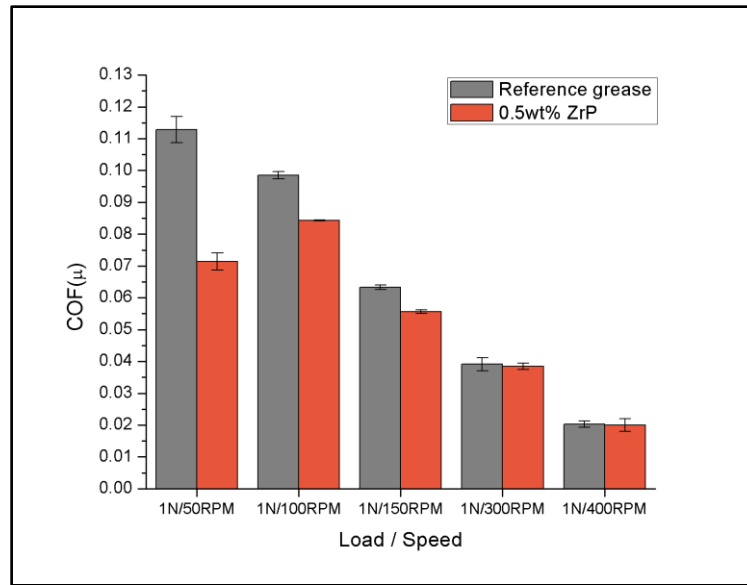


Figure 33. Comparison of the CoF at different rotating speeds

In the frictional performance on lubrication of grease, the addition of α -ZrP NPs shows the decrease of the CoF under different loads and at rotating speeds below 150RPM. These results can be explained with the opportunity for the decrease of friction with rotating and sliding of α -ZrP NPs.

5. 1. 4. Effects on frictional behavior at high temperature

The working temperature of a wind turbine is estimated from -20°F (-28.89°C) to 300°F (148°C) depending on its service places such as sea and desert [44]. For the potential application in a wind turbine, the addition of α -ZrP should show the enhanced performance on lubrication of grease at elevated temperatures.

It was observed that the CoF at high temperature for the comparison of frictional behavior of grease. Figure 34 shows the CoF of the reference grease and the grease

with 0.5wt% α -ZrP NPs according to the increased temperature. The grease with 0.5wt% α -ZrP consistently shows the lower CoF than the reference grease at 25°C, 50°C, 100°C, 150°C, and 200°C, respectively. The average decrease in the CoF shows 8.6% with the addition of 0.5wt% α -ZrP in grease. Two samples simultaneously show the decrease in the CoF with the increased temperature. This phenomenon can be explained with the decreased viscosity of grease at a high temperature [49]. This indicates that α -ZrP NPs are thermally stable at high temperature. The thermal stability provided the opportunity for α -ZrP NPs to be able to rotate and slide in the contact area [55]. Similar to the experiment at room temperature, this phenomenon also reduced friction at high temperature.

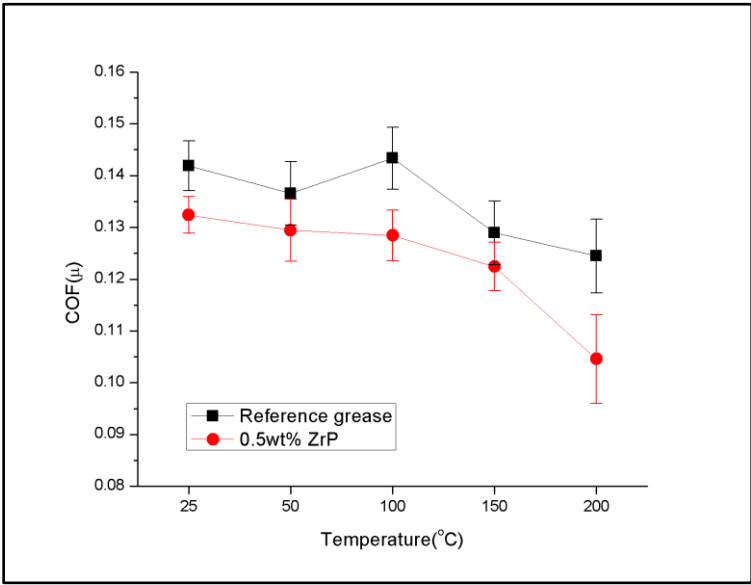


Figure 34. Comparison of the CoF with increased temperature

5. 2. Effects on wear

This section discusses about the wear resistance of grease that was significantly increased with the addition of α -ZrP NPs. In this section we analyze the wear scar and the wear track of worn surfaces after pin-on-disc tribometer experiments. The morphology of the wear scar and the wear track was characterized by optical microscope, interferometer and SEM.

5. 2. 1. Analysis of wear scar and wear track on worn surface

Figure 22 shows optical microscope (OM) images of the wear scar on ball bearings used in a pin-on-disc tribometer. The left figure clearly shows a larger area of worn scar than the right figure as marked with red circles. The reference grease developed a severe wear scar on the ball bearing, while the addition of α -ZrP NPs in grease protected the ball bearing from developing a severe wear scar.

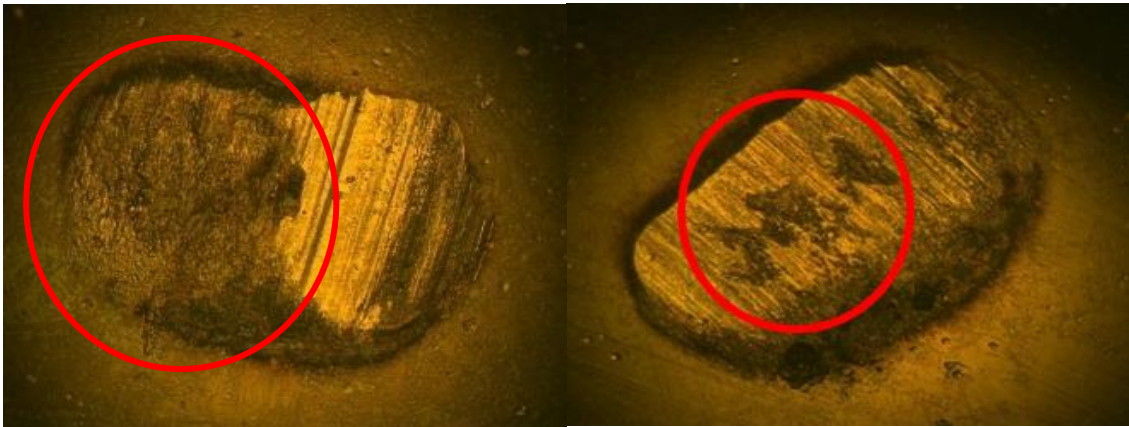


Figure 35. OM images of the wear scar of the reference grease (left) and α -ZrP (right)

Figure 23 shows the wear tracks of the reference grease and the grease with 0.5wt% α -ZrP after a pin-on-disc tribometer experiment for 2hours. In optical images, the dark color portion indicates the deformation of surfaces. When compared two images, the wear track of 0.5wt% α -ZrPNPs clearly shows the smaller dark portion than the reference grease. This means that the addition of α -ZrP NPs protected the surface from the deformation caused by friction and heat.

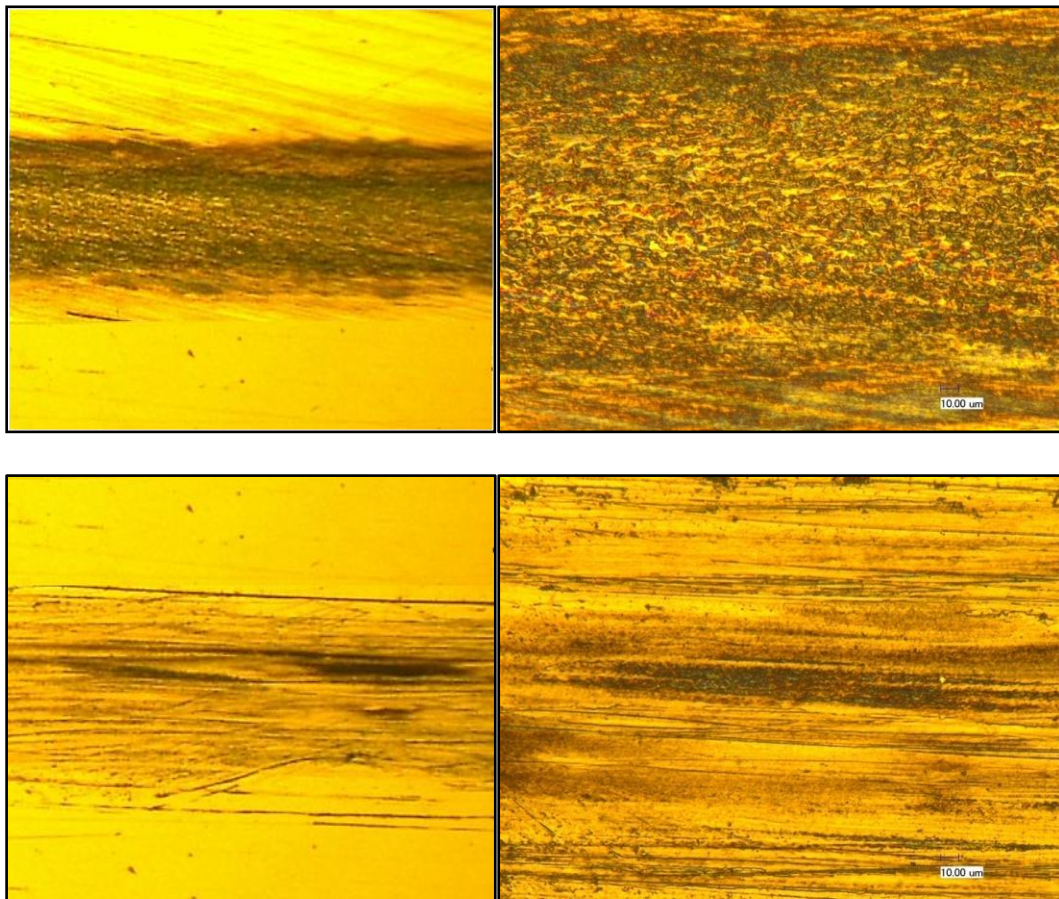


Figure 36. OM images of wear track of the reference grease (up) and α -ZrP (down)

Figure 24 show the 2D analysis images of a wear track using an interferometer. It clearly shows the narrow and shallow wear track in the right figure. A wear depth used for the calculation of wear volume was obtained from this 2D analysis. The detailed information of wear depth will be covered in the wear rate section.

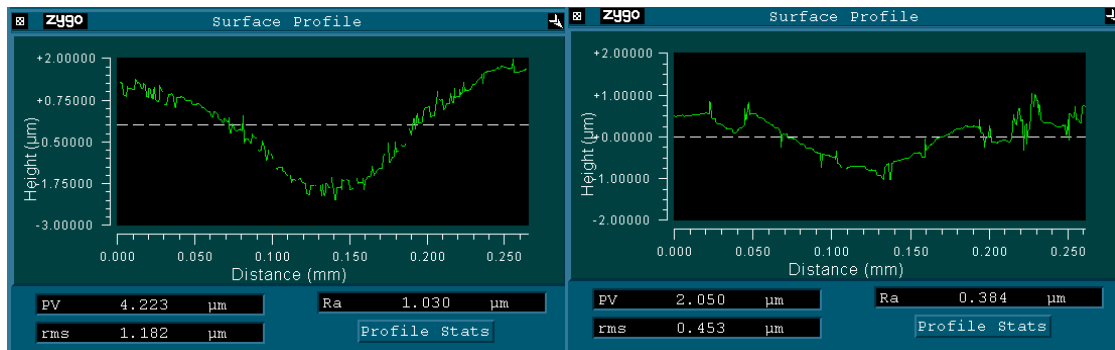


Figure 37. Interferometer results on the reference grease (left) and α -ZrP (right)

To study wear mechanisms, a scanning electron microscope (SEM) was used. Figure 38 are the surface morphology of wear tracks. As seen, the reference grease shows the plastic deformation of surfaces generated due to shear stress, contact pressure, and heat throughout the inner wear track, while the grease with α -ZrP shows the micro-cutting and the smaller portion of plastic deformation than the reference grease. In the case of the reference grease, the surface experienced fatigue due to high friction and temperature. However, the addition of α -ZrP protected the surface from developing fatigue with low friction.

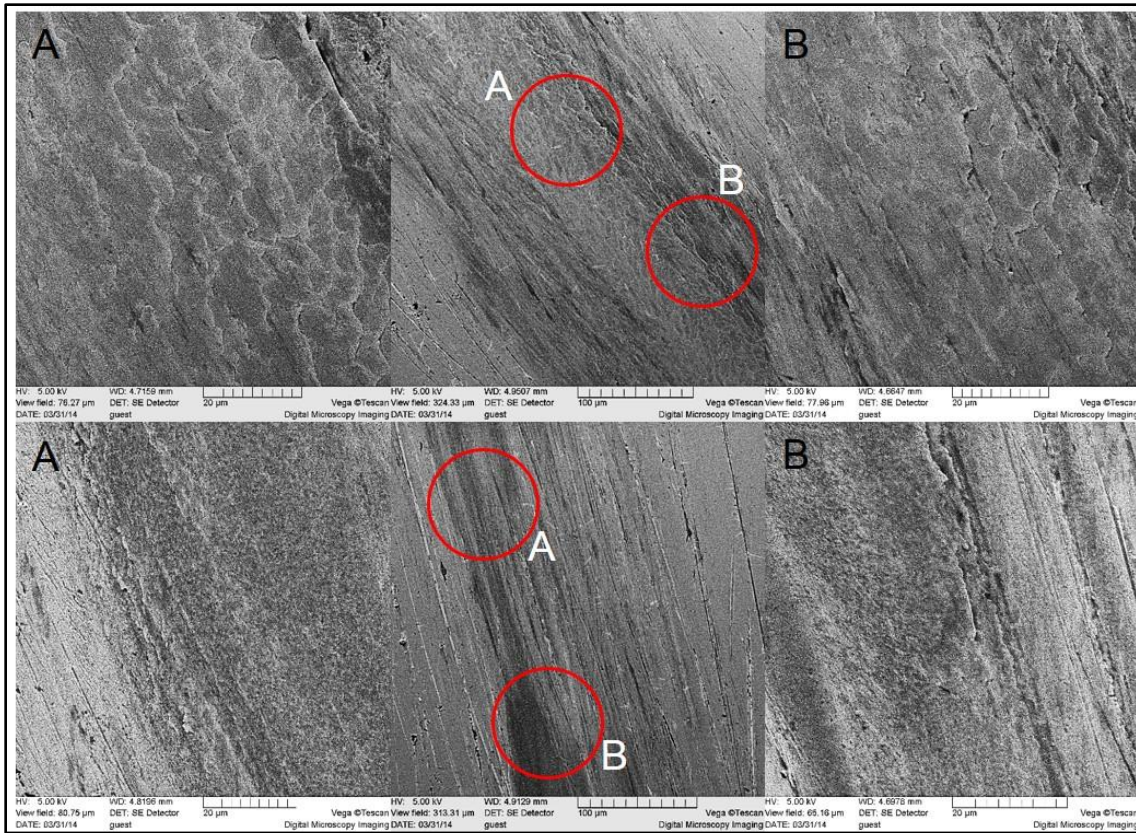


Figure 38. SEM images of wear track on the reference grease (up) and α -ZrP (down)

5. 2. 2. Analysis of roughness on worn surface

Figure 25 shows interferometer results with 2D and 3D analysis images. The roughness average of the grease with 0.5wt% α -ZrP is much lower than that of the reference grease. As shown in Table 12, the results show 1.097 μ m in the reference grease and 0.384 μ m in the grease with α -ZrP on an average of 3 different areas. The addition of α -ZrP NPs allowed not only to protect the surface from developing wear, but also to decrease the irregularity of sliding surface.

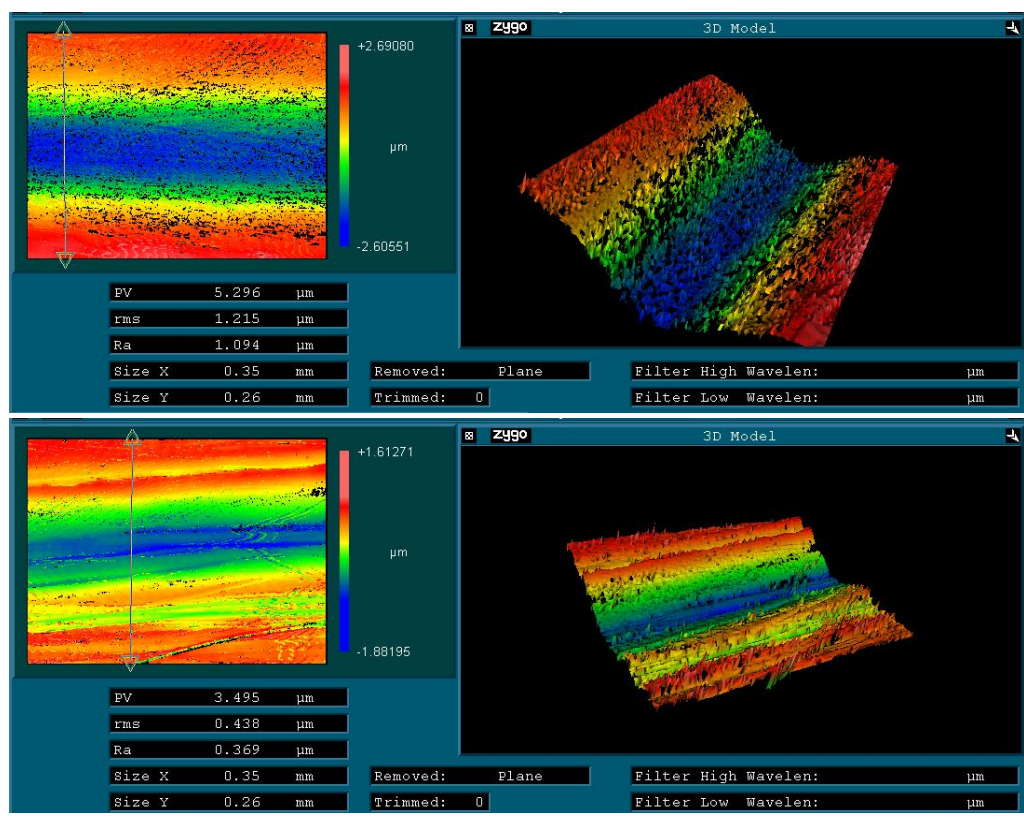


Figure 39. Interferometer results on the grease without (up) and with α -ZrP (down)

Table 12. Comparison of the roughness average

No.	Reference grease(μm)	0.5wt% α -ZrP(μm)
1	1.109	0.376
2	1.094	0.372
3	1.087	0.405
Average	1.097	0.384

5. 2. 3. Comparison of wear rate

From the optical microscope and interferometer results, the wear depth and width were measured to calculate the wear volume. Table 13 shows the result of the wear depth and width on worn surfaces. The average wear depth is 2.016 μm in the reference grease and 0.994 μm in 0.5wt% α -ZrP. In terms of the average wear width, the reference grease and the grease with 0.5wt% α -ZrP show 263.41 μm and 255.05 μm , respectively. The results indicate that the wear width is slightly decreased (~3.2%), while the wear depth is greatly decreased for 50% with the addition of α -ZrP NPs. This means that α -ZrP NPs contributed to the decrease in the wear depth rather than the decrease of the wear width.

Table 13. Comparison of wear depth and width

No.	Reference grease(μm)		0.5wt(%) α -ZrP added in grease(μm)	
	Wear Depth	Wear Width	Wear Depth	Wear Width
1	2.203	268.84	0.918	261.18
2	2.132	273.02	1.022	249.75
3	2.278	270.71	1.028	255.51
4	2.068	248.01	0.984	253.56
5	1.998	280.63	0.899	257.37
6	1.788	257.37	1.022	249.75
7	1.891	247.88	1.017	240.26
8	2.207	249.75	1.121	266.88
9	1.585	274.53	0.954	261.18
Average	2.016	263.41	0.994	255.05

As mentioned in Chapter III, a wear rate can be calculated by a wear volume, an applied load and a sliding distance. As a result of the calculation, the wear rate of the grease with 0.5wt% α -ZrP was significantly decreased for 52% than that of the reference grease, as shown in Figure 40. The performance of grease on the wear resistance was greatly improved with the addition of α -ZrP NPs. This significant improvement comes from the combination of NPs shape and layered structure of α -ZrP. First of all, the nanoplatelet shape of α -ZrP performs to protect the surface by rotating and sliding, as described in the frictional behavior part. In addition, the double-layered structure of α -ZrP is expected for them to slide. The exfoliated layer is smaller than the height of asperity. Subsequently, asperities acted as reservoirs which cover the surfaces [56]. This means that the addition of α -ZrP effectively decreased the contact of asperities due to the sliding and rotating motions. Further analysis will be discussed in a later section.

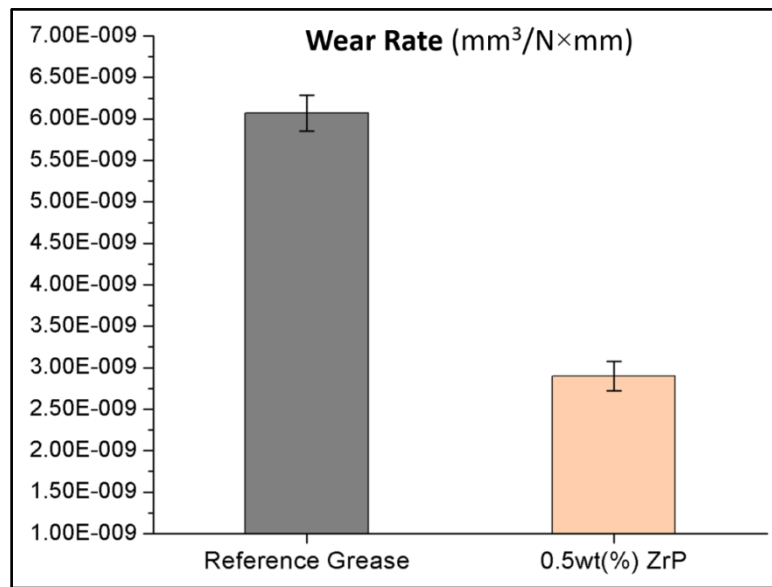


Figure 40. Comparison of wear rate

As shown in Figure 41, the CoF of the reference grease was significantly increased after 200 seconds running in period, while the grease with 0.5wt% α -ZrP NPs didn't induce visible change in the CoF during the 2hr experiment. When friction is significantly higher, the sliding surfaces are expected to wear. On the other hand, the grease with α -ZrP NPs kept the surfaces smooth without any severe wear. The analysis of morphology of wear track can be a proof of this explanation.

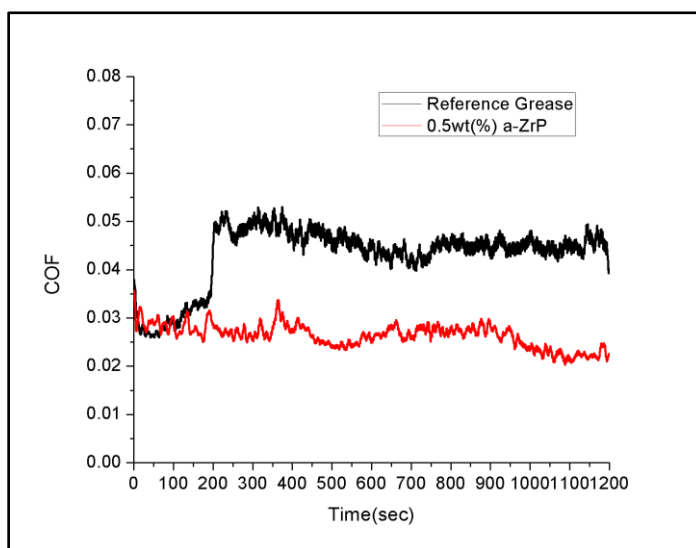


Figure 41. Friction response for 2 hours in tribometer experiment

5. 3. Effects on galling resistance

In terms of galling resistance, the grease shows the reduced frictional behavior and the acceptable galling level with α -ZrP under high load. In this research, API RP 7A1 experiment was conducted for the observation on the galling resistance of grease.

Once all experiments were completed, visual inspection and data analysis were carried out.

5. 3. 1. Visual inspection

The substrate with grease was inspected by the naked eye after all experiments. As shown in Figure 27, the reference grease and the grease with 0.5wt% α -ZrP didn't develop any severe galling traces between sliding surfaces. All substrates met the level 1 or 2 in the classification of galling level. This observation can be a proof that the grease with α -ZrP is acceptable as a lubricant.

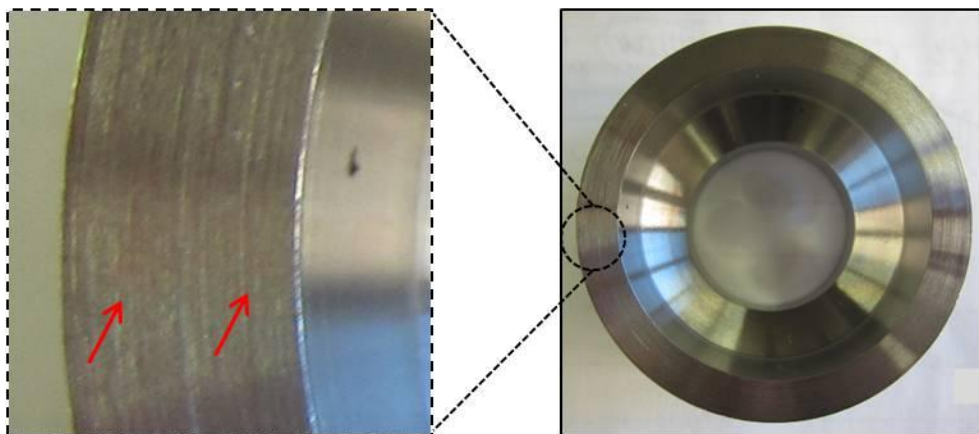


Figure 42. No galling traces on a substrate after API RP 7A1 experiment

5. 3. 2. Data analysis

Data analysis is comprised of the torque versus turns plot analysis and the comparison of friction factor. The make-up torque and the break-out torque versus rotation degrees were plotted to inspect the existence of gall on sliding surfaces during

all experiments. As shown in Figure 43, all results of the grease with 0.5wt% α -ZrP indicate that the make-up torque (black line) is clearly upper than the break-out torque (red line) in all experiment results. Thus, the grease with 0.5wt% α -ZrP performed properly to lubricate sliding surfaces without any severe adhesion.

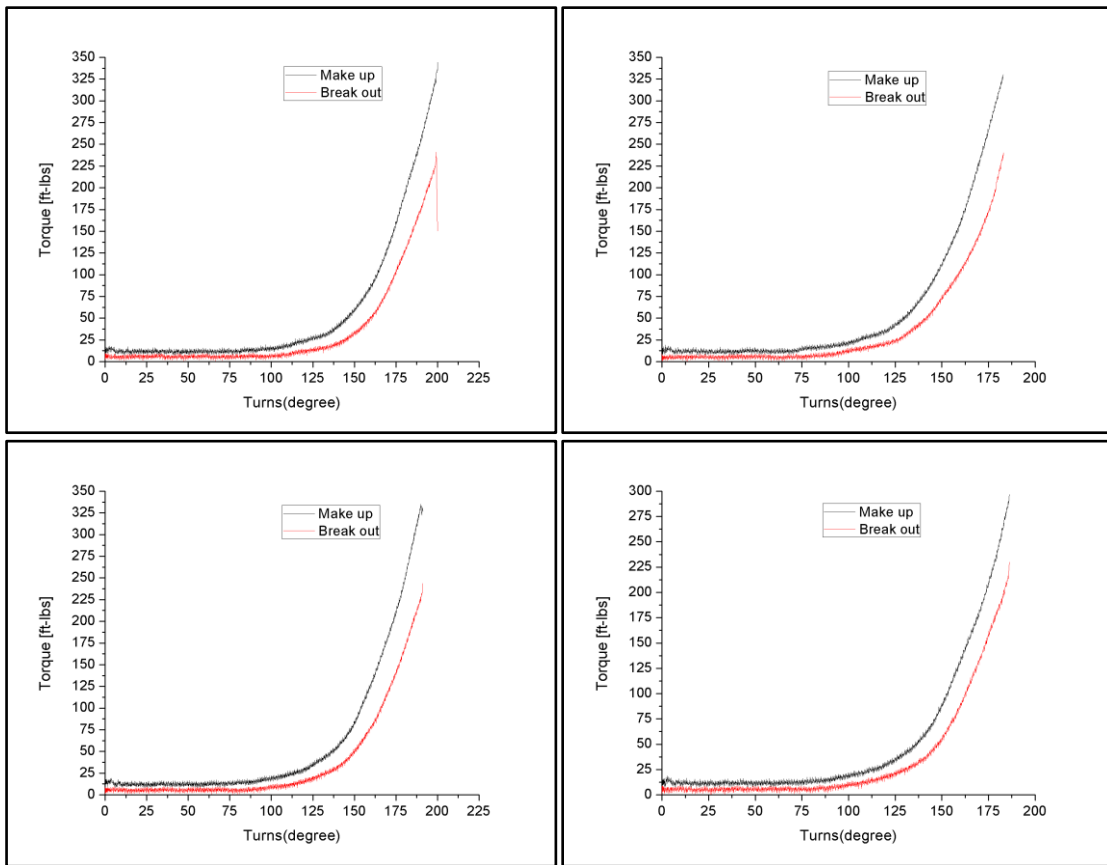


Figure 43. Make-up and break-out versus rotation degree plots for α -ZrP

A friction factor is used to convert the relative frictional behavior of grease for the absolute evaluation by using the reference compound [51]. As shown in Table 11, the friction factor of the reference grease is 1.261 and that of the grease with 0.5wt% α -

ZrP NPs is 1.228. In the comparison of the friction factor, the grease with 0.5wt% α -ZrP NPs shows the improved frictional behavior of 2.62% under high load (up to 55,000pounds). This result can be explained by the shape of nanoplatelets. As described in Chapter I, nanoplatelets experiences the least pressure under an applied load. In addition, the high load bearing capability of α -ZrP has been reported [57]. As a result, the addition of α -ZrP NPs in grease shows the enhanced frictional behavior without the adhesion of surfaces under high pressure.

Table 14. Slope of line on the reference grease and the grease with 0.5wt% ZrP

	1 st reference compound	0.5wt% α -ZrP	2 nd reference compound	1 st reference compound	Super Lube	2 nd reference compound
1	3.67	4.47	3.7	4.19	4.45	3.97
2	3.7	4.67	3.67	3.93	5.42	3.82
3	3.54	4.43	3.45	4.06	4.5	3.69
4	3.35	4.2	3.56	4.12	4.58	3.48
5	3.55	4.22	3.56	3.87	4.11	3.49
Average	3.56	4.39	3.59	3.63	4.61	3.69
Friction factor	1.228			1.261		

5. 4. Mechanism of α -ZrP NPs on lubrication of grease

The experimental results of this research represent the reduced friction and wear with the addition of α -ZrP in grease. Two mechanisms can be proposed: the nanoplatelet shape and the layered structure.

The first explanation on the enhanced lubrication of the grease with α -ZrP comes from the shape of nanoplatelets. As depicted in Figure 29, α -ZrPNPs could rotate and slide in the contact area [56-59]. The rotating and sliding motions of nanoplatelets decreased the direct contact of asperities on the mating surfaces. Subsequently, the cold-welding of asperities which cause the deformation of surface was restrained, and friction was decreased with the low shear stress [30]. In addition, the alignment of α -ZrP NPs under an applied pressure reinforced the effect of such behavior [49].

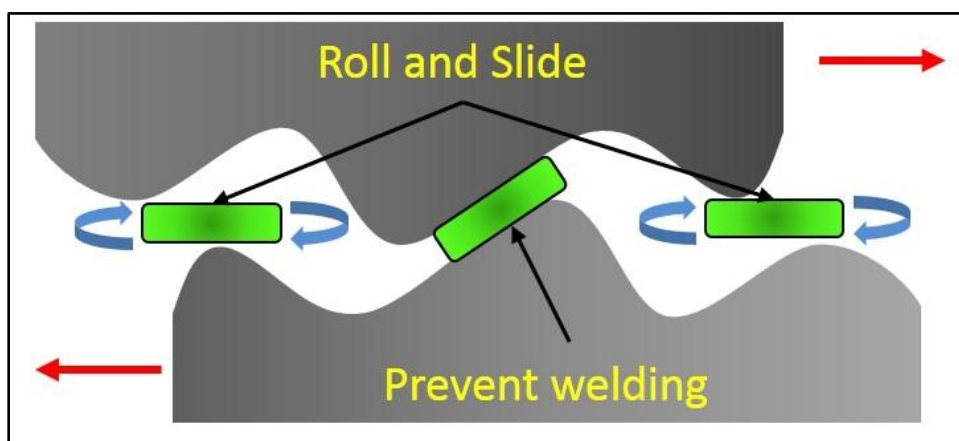


Figure 44. Illustration of the role of α -ZrP NPs between sliding surfaces

The second mechanism relates to the layered structure of α -ZrP. In α -ZrP, zirconium atoms connect to phosphate groups via oxygen atoms and form the layered structures atomically with 6.6\AA in thickness [48]. The layer is bonded parallel to the adjacent layer by Hydrogen bonds and between each layers, the space maintains at 7.6\AA , as described in Figure 45 [60]. The relatively weak Hydrogen bond between adjacent atomic layers enables them to be exfoliated under a shearing force.

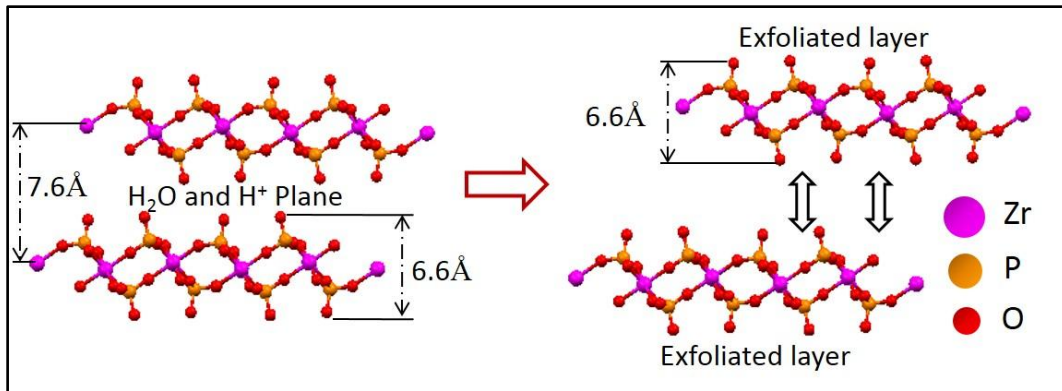


Figure 45. Exfoliated layers of α -ZrP [60]

The exfoliated layers are easily trapped within the valleys of asperities which can act as physical barriers [59]. Thus, α -ZrP NPs can stay in the area between asperities of the shearing surfaces and change the shear line with artificially smoothing out the surface, as depicted in Figure 46.

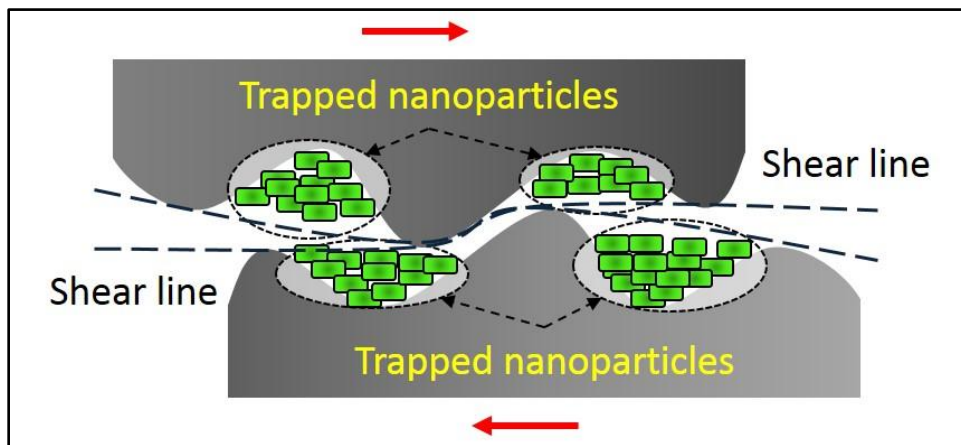


Figure 46. Illustration of the change of the shear line by trapped nanoparticles

The nanoplatelet shape and the layered structure of α -ZrP were significantly improved the frictional behavior and the wear resistance on lubrication of grease. In addition, the high thermal stability of α -ZrP maintained the shape and the structure of α -ZrP NPs at high temperature. These effects are essential to be acceptable in industrial machinery for improving the efficiency and lifetime.

CHAPTER VI

CONCLUSION AND FUTURE RECOMMENDATIONS

6. 1. Conclusions

The tribological performance of nanomaterial-enhanced quasi-liquid lubricant (grease) was investigated using a pin-on-disc configuration and galling experiments under various experiment conditions. Two different nanomaterials were studied: yttrium oxide and α -phase zirconium phosphate. Analysis showed that yttrium oxide and zirconium phosphate represented two-dimensional (2D) nanostructures.

There are three main findings in this research:

- 1) Two-dimensional nanomaterials enhanced the frictional behavior of grease at elevated temperature. In addition, the lowest coefficient of friction was shown with 0.5wt% of concentration nanoparticles in grease. The enhanced frictional behavior was investigated with the sliding and rotating movements of 2D nanopartilces. Friction was found decreased due to the alignment of 2D nanoparticles during sliding.
- 2) Wear study indicated that the wear resistance was significantly increased with the addition of zirconium phosphate, while yttrium oxide didn't show improvement. Furthermore, zirconium phosphate in grease could protect surfaces from the deformation and severe wear.
- 3) Galling experiments revealed that the grease with nanomaterials as additives was suitable as a lubricant. Data analysis showed that zirconium phosphate

enhanced the galling resistance of grease with the decreased friction factor, while yttrium oxide otherwise. The combination of the particle shape and the lamellar structure offered an effective solution for lubrication under extreme pressure.

This research offers alternative solutions for lubrication design and development that are beneficial for applications in particular in wind turbines, and other high performance machineries. .

6. 2. Future recommendations

It is suggested that investigation is carried out in order to understand the mechanisms of nanomaterials as lubricant additives.

More and detailed characterization is suggested at the atomic level in order to obtain better understanding in effects of nanomaterials that enhance lubrication.

REFERENCES

- [1] Williams, J. A., 2005, *Engineering Tribology*, Cambridge University Press, Cambridge, UK, pp. 12-38.
- [2] Kelly, K., 2009, *Early Civilizations: Prehistoric Times to 500 C.E. (History of Medicine)*, Ferguson Publishing Company, New York, NY, pp. 13-26.
- [3] Kathryn, C., Robert, G. M., Neil, C., and Michael, A., 2005, "The Ten Greatest Events in Tribology History," *Technology & Lubrication Technology*, **61**, pp. 38-39.
- [4] Mang, T., and Dresel, W., 2007, *Lubricants and Lubrication*, Wiley-VCH, Germany, pp. 68-94.
- [5] Black, C. C., and Heaton, C., 2004, *Leonardo da Vinci and His Works: Consisting of a Life of Leonardo da Vinci*, Kessinger Publishing, Whitefish, Montana.
- [6] Seirig, A., 1998, *Friction and Lubrication in Mechanical Design*, CRC Press, Boca Raton, FL, pp. 224-289.
- [7] Jurgen, H., and Kappl, M., 2010, *Surface and Interfacial Forces*, Wiley-VCH, Germany.
- [8] Gohar, R., and Rahnejat, H., 2008, *Fundamentals of Tribology*, Imperial College Press, London, UK.
- [9] Stachowiak, G. W., 2005, *Wear: Materials, Mechanisms and Practice*, John Wiley and Sons, London, UK.
- [10] Buckley, D. H., 1981, *Surface Effects in Adhesion, Friction, Wear, and Lubrication*, Elsevier Science, New York, NY, pp. 246-312.
- [11] Bayer, R. G., 2004, *Engineering Design for Wear*, CRC Press, Boca Raton, FL, pp. 98-134.
- [12] Fischer, A., and Bobzin, K., 2011, *Friction, Wear and Wear Protection*, Wiley-VCH, Germany, pp. 1-19.
- [13] ASTM book of standards, 1987, "Corrosion," ASTM International, Pennsylvania.
- [14] Cundari, T. R., and Lipkowitz, K. B., 2007, *Reviews in Computational Chemistry*, Wiley-VCH, Germany, Chap. 4.

- [15] Mortier, R. M., Fox, M. F., and Orszulik, S. T., 2009, *Chemistry and Technology of Lubricants*, Springer, New York, NY.
- [16] Johnson, M., 2008, "Selecting the Correct Lubricant for Element Bearings," *Tribology & Lubrication Technology*, Park Ridge, IL.
- [17] Mellage, C., Fugate, D., Grigar, E., Agashe, G., Doskow, K., and Mahecha, L., 2012, "Global Lubricant Consumption-Where Are We Going?," Kline Blog, <http://blogs.klinegroup.com/2012/01/04/global-lubricant-consumption-where-are-we-going> (accessed April 29, 2014)
- [18] American Petroleum Institute, 2012, "Engine Oil Licensing and Certification System," 17th Edition, API, Washington, D. C.
- [19] Herguth, B., 2002, "Grease Analysis-Monitoring Grease Serviceability and Bearing Condition," *Practicing Oil Analysis*, <http://www.machinerylubrication.com/Read/296/grease-analysis> (accessed April 28, 2014)
- [20] Archbutt, L., and Deeley, R. M., 1907, *Lubrication and Lubricants: A Treatise on the Theory and Practice of Lubrication, and on the Nature, Properties, and Testing of Lubricants*, C. Griffin and Company, London, UK, Chap. 2.
- [21] Wright, J., 2008, "Grease Basic," *Machinery Lubrication*, <http://www.machinerylubrication.com/Read/1352/grease-basics> (accessed April 28, 2014)
- [22] Johnson, M., 2008, "Understanding grease construction and Function," *Tribology & Lubrication Technology*, https://www.stle.org/assets/document/1Grease_construction_and_function.pdf (accessed April 28, 2014)
- [23] Christiernsson, A., 2004, "The Chemistry and Physics of Grease, The Advantages of Grease," White Paper Lubrisense, AXEL, Sweden.
- [24] Sumerlin, S., 2010, "The Rights and Wrongs of Greasing: From Selection to Application," *Machinery Lubrication*, <http://www.machinerylubrication.com/Magazine/Issue/Machinery%20Lubrication/3/2010> (accessed April 28, 2014)
- [25] Rudnick, L. R., 1992, *Synthetics, Mineral Oils, and Bio-Based Lubricants*, CRC Press, Boca Raton, FL, pp. 3-373.

- [26] Jackson, A., 1987, "Synthetic versus Mineral Fluids in Lubrication," International Tribology Conference, Princeton, UK.
- [27] Johnson, M., 2008, "Understanding grease construction and function," Tribology & Lubrication Technology, Park Ridge, FL.
- [28] Britannica, 2008, "Lubrication," The Encyclopaedia Britannica, <http://www.britannica.com/EBchecked/topic/350437/lubrication/4346/Oiliness> (accessed April 28, 2014)
- [29] Silverstein, R., and Rudnick, L. R., 2009, *Lubricant Additives*, CRC Press, Boca Raton, FL, Chap. 23.
- [30] Akbulut, M., 2012, "Nanoparticle-Based Lubrication Systems," Powder Metallurgy & Mining, College station, TX.
- [31] Eranna, G., 2011, *Metal Oxide Nanostructures as Gas Sensing Devices*, CRC Press, Boca Raton, FL, pp. 1-6.
- [32] Rao, C. N. R., Muller, A., and Cheetham, A. K., 2005, *The Chemistry of Nanomaterials*, Wiley-VCH, Germany, pp. 1-11.
- [33] Belmilouda, N., Mertens, P. W., Tamaddon, A. H., Xu, X., and Struyf, H., 2011, "Investigation on the Drying Dynamics of Millimetric Water Droplets: Source of Watermarks on Silicon Wafers," The Electrochemical Society, **41**, pp. 205-212.
- [34] Rai, A., Park, K., Zhou, L., and Zachariah, M. R., 2006, "Understanding the Mechanism of Aluminum Nanoparticle Oxidation," Combustion Theory and Modeling, **10**(5), pp. 843-859.
- [35] Kim, Y. S., and Liang, H., 2013, "Active Nano-structured Composite Coatings for Corrosion and Wear Protection of Steel," M. S. Thesis, Texas A&M university, College Station, TX.
- [36] Chou, C. C., and Lee, S. H., 2010, "Tribological Behavior of Nanodiamond-Dispersed Lubricants on Carbon steels and Aluminum alloy," Wear, **269**(11-12), pp. 757-762.
- [37] Cizaire, L., Vacher, B., Mogine, T. L., Matine, J. M., and Tenne, R., 2002, "Mechanisms of Ultra-low Friction by Hollow Inorganic Fullerene-like MoS₂ Nanoparticles," Surface and Coatings Technology, **160**(2-3), pp. 282-287.

- [38] Kao, M. J., and Lin, C. R., 2009, "Evaluating The Role of Spherical Titanium Oxide Nanoparticles in Reducing Friction between Two Pieces of Cast Iron," *Journal of Alloys and Compounds*, **483**(1-2), pp. 456-459.
- [39] Choi, Y., Lee, C., Hwang, Y., Park, M., Lee, J., Choi, C., and Jung, M., 2009, "Tribological Behavior of Copper Nanoparticles as Additives in Oil," *Current Applied Physics*, **9**(2), pp. e124-e127.
- [40] Mukhopadhyay, A., 2011, "Tribology: A Potential Source of Energy Savings in Industry," *Propagation*, Kolkata, India.
- [41] Bhushan, B., 2000, *Modern Tribology Handbook*, CRC Press, Boca Raton, FL, pp. 205-312.
- [42] Brazen, D., 2009, "Lubrication of Wind Turbines," *Kansas Renewable Energy*, Kansas.
- [43] Applied Industrial Technologies, 2009, "Lubricant Failure=Bearing Failure," *Machinery Lubrication*, <http://www.machinerylubrication.com/Read/1863/lubricant-failure>
- [44] Holm, A. P., 2009, "Specialty Lubricants for Optimum Operation," *Wind systems*, Alabama.
- [45] Liu, R., and Li, D. Y., 2000, "Effects of yttrium and cerium additives in lubricants on corrosive wear of stainless steel 304 and Al alloy 6061," *Journal of Materials Science*, **35**(3), pp. 633-641.
- [46] He, X., Xiao, H., Kyle, J. P., Terrell, E. J., and Liang, H., 2013, "Two-dimensional Nanostructured Y₂O₃ Particles for Viscosity Modification," *Applied Physics Letters*, **104**(16).
- [47] Warmuth, W. M., and Schollhorn, R., 1994, *Progress in Intercalation Research*, Kluwer Academic Pub, Norwell, MA, pp. 102-134.
- [48] Sun, L., Boo, W. J., Sue, H. J., and Clearfield, A., 2007, "Preparation of α -ZrP Nanoplatelets with Wide Variations in Aspect Ratios," *New Journal of Chemistry*, **31**, pp. 39-43.
- [49] He, X., Xiao, H., Choi, H. H., Diaz, A., Mosby, B., Clearfield, A., and Liang, H., 2014, "a-Zirconium Phosphate Nanoplatelets as Lubricant Additives," *Colloids and Surfaces*, **452**, pp. 32-38.

- [50] Kim, J. H., 2013, "Boron-based Additives in Oil and Grease for Wind Turbine Applications," M. S. Thesis, Texas A&M university, College Station, TX.
- [51] American Petroleum Institute, 1989, "Friction and Galling Resistance Property test for Thread Compounds," API, Washington, D. C.
- [52] American Special Metals Corporation, 2014, "Inconel Alloys," ASM Cor., <http://www.americanspecialmetals.com/InconelAlloys.html> (accessed May 11, 2014)
- [53] Special Metals, 2007, "Inconel Alloy 718," Special Metals Corporation, <http://www.specialmetals.com/documents/Inconel%20alloy%20718.pdf> (accessed May 11, 2014)
- [54] Carignan, F. J., and Knoth, B. H., 1989, "High-temperature Tribometer," Advanced Mechanical Technology, Newton, Kansas.
- [55] Yuan, Z. Y., Ren, T. Z., Azioune, A., Pireaux, J. J., and Su, B. L., 2005, "Marvelous Self-assembly of Hierarchically Nanostructured Porous Zirconium Phosphate Solid Acids with High Thermal Stability," *Catalysis Today*, **105**(3-4), pp. 647-654.
- [56] Yadgarov, L., Petrone, V., Rosentsveig, R., Feldman, Y., Tenne, R., and Senatore, A., 2013, "Tribological studies of rhenium doped fullerene-like MoS₂ nanoparticles in boundary, mixed and elasto-hydrodynamic lubrication conditions," *Wear*, **297**(1-2), pp. 1103-1110.
- [57] Liu, L., Chen, Z. F., Wei, H. B., and Dong, J. X., 2010, "Inonothermal Synthesis of Layered Zirconium Phosphates and Their Tribological Properties in Mineral Oil," *Inorganic Chemistry*, **49**(18), pp. 8270-8275.
- [58] Greenberg, R., Halperin, G., Etsion, I., and Tenne, R., 2004, "The Effect of WS₂ Nanoparticles on Friction Reduction in Various Lubrication Regimes," *Tribology Letters*, **17**(2), pp. 179-186.
- [59] Pottuz, L. J., Dassenoy, F., Belin, M., Vacher, B., Martin, J. M., and Fleischer, N., 2005, "Ultralow-friction and Wear Properties of IFWS₂ under Boundary Lubrication," *Tribology Letters*, **18**(4), pp. 477-485.
- [60] Diaz, A., Saxena, V., Gonzalez, J., David, A., Casanas, B., Clearfield, A., and Hussain, M. D., 2012, "Zirconium Phosphate Nanolatelets: A Novel Platform for Drug Delivery in Cancer Therapy," *Chem. Commun.*, **48**, pp. 1754-1756.